



UNIVERSITY OF LEEDS

This is a repository copy of *A review of experimental and analytical studies on the out-of-plane behaviour of masonry infilled frames*.

White Rose Research Online URL for this paper:
<http://eprints.whiterose.ac.uk/156346/>

Version: Accepted Version

Article:

Anić, F, Penava, D, Abrahamczyk, L et al. (1 more author) (2020) A review of experimental and analytical studies on the out-of-plane behaviour of masonry infilled frames. *Bulletin of Earthquake Engineering*, 18 (5). pp. 2191-2246. ISSN 1570-761X

<https://doi.org/10.1007/s10518-019-00771-5>

© Springer Nature B.V. 2019. This is a post-peer-review, pre-copyedit version of an article published in *Bulletin of Earthquake Engineering*. The final authenticated version is available online at: <http://dx.doi.org/10.1007/s10518-019-00771-5>

Reuse

Items deposited in White Rose Research Online are protected by copyright, with all rights reserved unless indicated otherwise. They may be downloaded and/or printed for private study, or other acts as permitted by national copyright laws. The publisher or other rights holders may allow further reproduction and re-use of the full text version. This is indicated by the licence information on the White Rose Research Online record for the item.

Takedown

If you consider content in White Rose Research Online to be in breach of UK law, please notify us by emailing eprints@whiterose.ac.uk including the URL of the record and the reason for the withdrawal request.



eprints@whiterose.ac.uk
<https://eprints.whiterose.ac.uk/>

Literature Review of Research on Out-of-Plane Behaviour of Masonry Infilled Frames

Consituting of experimental and analytical studies

Filip Anić · Davorin Penava · Lars Abrahamczyk ·
Vasilis Sarhosis

Received: date / Accepted: date

Abstract This paper presents a literature review of research done on the out-of-plane behaviour of masonry infilled frames. This paper also reckoned the effects of bidirectional loads, openings, slenderness, boundary conditions and etc. As it was found by numerous researchers that those effects play a crucial role in achieving arching-action cause they can bypass or limit its effectiveness. Namely, arching-action develops additional compressive forces that resist the traversal ones. Such is evident with inertial methods of testing, while the same can not be stated for inter-storey drift or dynamical methods. It is to be acknowledged that most experimental test were done using the inertial methods, mostly with the use of air-bags. In contrast, only few were done with dynamical and only two with inter-storey drift methods. It was found that inertial and inter-storey drift methods differ widely. Particularly, inertial methods damage the infill, leaving the frame more or less intact. Contrariwise, drift damages the frame, while infill, only slightly. Openings were investigated; however, with contrasting results. Namely, all found that openings do lower the deformational but not all load-bearing capacities. Furthermore, analytical models have shown disperse results among themselves and with experimental data. Models stabilities were checked with single- and multi-variable parametric analysis with few limitations intensified. Also, the governing factors, influences of frame and other parameters were found.

Keywords Out-of-plane · experimental studies · analytical studies · infilled frames · masonry infill

1 Introduction

Earthquakes are natural occurring phenomena's that manifest themselves by shaking and displacing the ground. Buildings in those areas are considered to have a certain degree of seismic vulnerability. Above all, it is common for high-rise, i.e. multi-storey buildings to retain a comparably higher degree of seismic vulnerability. Thus, in order to understand and lower the seismic vulnerability, a separate field of structural engineering developed titled earthquake or seismic engineering. The field began by some sources early as 1876's (Howe, 1936) and it is still ongoing to this day. It contributed to various cognitions and provisions, termed *anti-seismic regulations for civic and building protection*. Some provisions are regulated nationally, and some internationally. List of such provisions are shown on Table 1. Whereas, Table 1 leads to the conclusion that all codes are more or less intertwined, with majority of codes based upon ACI (2011) provisions from United Stated.

Majority of high-rise, i.e. multi-storey buildings have their structural load-bearing framework made either of reinforced concrete (RC) or structural steel (SS) with some sort of non-bearing infill wall/panel.

F. Anić
Vladimir Prelog street 3, Osijek, Croatia
E-mail: filip.anic@gfos.com

D. Penava
Vladimir Prelog street 3, Osijek, Croatia

L. Abrahamczyk
Marienstraße 7A, Weimar, Germany

V. Sarhosis
Drummond Building, Newcastle upon Tyne, United Kingdom

Table 1: Worldwide seismic building codes

#	Code	Remark
1	European standards BSI (2005)	
2	American Concrete Institute ACI-318 ACI (2011)	
3	Applied Technology Council (ATC) – Federal Emergency Management Agency (FEMA 273 & 356) FEMA 273 (1997); FEMA 356 (2000)	
4	The Indian Standards on Earthquake Engineering IS IS 1893 (2002)	
5	Peruvian Tehnical standard of building E.030 NTS (1997)	
6	Chilean Nch433 NCH (1996)	Based upon ACI-05
7	Ecuadorian INEN-5 INEN (2001)	Based upon ACI-318-71
8	Nepal National Building Code NBC-105 MHPP (1995)	Largely following IS Code
9	Colombian Standards for Seismic Resistant Design and Construction NSR-84 CAEE (1984)	Based upon ACI
10	National Structural Code of Philippines, Vol. 1, Fourth Edition (NSCP) NSCP (1992)	Based upon ACI
11	New Zeland: Code of Practice for the Design of Concrete Structures, Part 1 (NZS-3101) NZS-3101 (1995)	
12	Israeli: Design Provisions for Earthquake Resistance of Structure (SI-413) SI (1995)	
13	Russian: Building Code on Construction in Seismic Areas (SNiP-II-7–81) SNiP (1995)	
14	Venezuelan Seismic Code, 1988. Regulations for Earthquake Resistant Buildings CNIC (1988)	
15	Vietnamese seismic design standard TCXDVN 375: 2006 VBS (2006)	Based upon SNiP
16	Canadian Standards Association and Standards Council of Canada	

In South Europe, the traditional structural systems are composed of RC frames with non-bearing unreinforced masonry walls (URM) (Booth and Key, 2006), in further text referred as *infill*. Most commonly, hollow clay blocks are used as a infill units. They possesses better thermal properties, greater shear strength and work efficiency than solid bricks. Most often, blocks are stacked with voids facing vertically. However, the traditions in west, as in Portugal, blocks are laid so the voids are facing horizontal direction (de Sousa, 2014).

When subjected to ground motions, structures are prone to inertial and inter-storey drift forces (Fig. 2). With infilled frame structures, the inter-storey drift forces are transmitted as displacements trough rigid diaphragms. i.e. slabs. While the inertial forces are the consequence of accelerated higher masses, predominately of the infill. Therefore, the inertial failures are expected at higher storeys and with infills that have less connections in their boundary conditions. Greater inter-storey drift damages are expected at lower storeys, where the shear forces are greater, along with additional reduction of infill’s inertial characteristics from gravity loads of upper storeys. Most commonly, the inter-storey drift damages are observable by the heavy cracking of the frame and by the development of plastic hinges (Fig. 2a, 2b). Damages from inertial forces are observable by heavy cracking of the infill and frequently, by missing larger parts of the wall (Fig. 2e-2c).

During ground motion excitations, infill interacts with the surrounding frame; thus, rendering its behaviour and with it, the behaviour of whole structure. Due to its complex problem, this interaction is yet to be implemented in European seismic codes (BSI, 2005). Hence, it is one of the most popular researched subjects in the field. Specifically, it was known from early 60’s (McDowell et al., 1956b; Holmes, 1961) that infill does contribute to the overall behaviour of frames. However, a way to implement the interaction is still thoroughly researched and at the time of code development, largely unknown. Therefore; with limited information, Eurocode 8 (BSI, 2005), regards infill as a secondary element during ground motions. Accordingly, this resulted in a more redundant frames.

In order to better comprehend the complex problem of the frame-infill interaction, many studies were conducted since the early 60’s. The field broaden and divided into four main components, listed by prevalence:

1. In-Plane (IP), where the frames are loaded in the direction of their axial plane;
2. Out-of-Plane (OoP) where the frames are loaded perpendicularly to their axial plane;
3. Bidirectional (IP+OoP, OoP+IP and simultaneous).

The IP+OoP describes OoP behaviour due to previous IP damage, and OoP+IP vice versa. Simultaneous action describes a synchronous IP and OoP loading protocol.

Furthermore, greatest focus was held on the field of IP, less in field of OoP and scarcely for the bidirectional behaviour (Asteris et al., 2017). In recent years, OoP research is gaining momentum (Fig. 1) in experimental surveys (Tab. 2-4), micro- (Reindl et al., 2011; Yuen and Kuang, 2012), macro- (Al Hanoun et al., 2018; Furtado et al., 2016) and analytical modelling (Tab 6, Fig. 1).

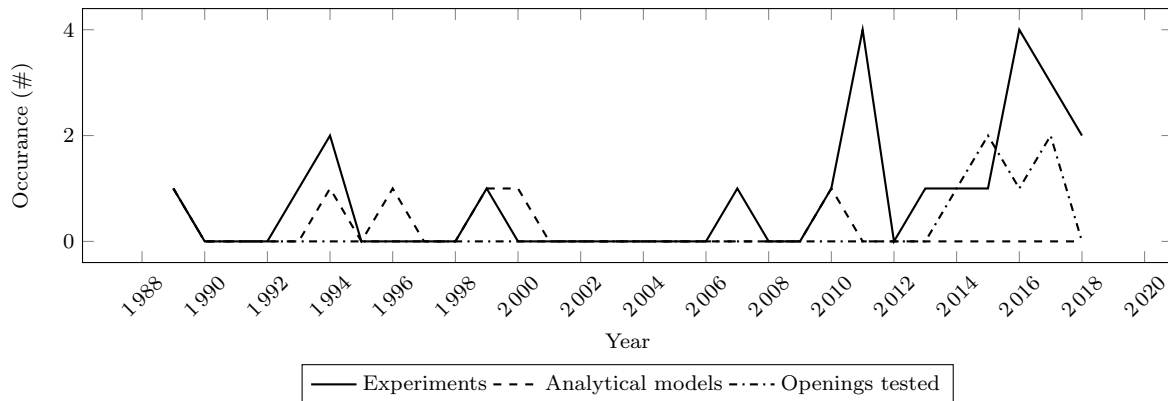


Figure 1: Occurrences of OoP specific subjects by year published

Regarding the aspect of seismic codes on OoP behaviour, Eurocode 8 (BSI, 2005) provisions only restrict the OoP collapse of slender infills (if $h/t > 15$). It states that in case of slender infill, special actions are required, such as application of: light wire meshes, wall ties fixed to the columns, wind posts and concrete belts (BSI, 2005). U.S. codes of Masonry Standards Joint Committee Committee et al. (1999) propose a calculation of OoP load-bearing capacity with the use of Dawe and Seah (1989) equations (Eq. 3, 4). On the other side, Canadian code (Canadian Standards Association and Standards Council of Canada, 1978) does not include specific method of obtaining the OoP capacity. However, it states that arching-action (Sec. 2.1) method should be used. US Federal recommendations FEMA 356 (2000); FEMA 273 (1997) and those that are based upon FEMA, as New Zealand codes (NZS-3101, 1995) use the approaches to assets OoP damage types and calculations of OoP bearing capacity (Eq. 8) that are simplified version of equation found by Angel et al. (1994) (Eq. 5).

First studies that researched the OoP behaviour of infill walls where not from seismic; rather, blast engineering field. The pioneering work was done by the *Armour research foundation* sponsored by U.S. Air Force, with authors such as McDowell et al. (1956b,a) and Monk (1958). In blast engineering, the OoP load is introduced by the explosions blast waves that pressurise the infill. Hence, the experimental work was done with infill's pressurisation, most commonly with air-bags. Blast engineers laid the ground work for the field of seismic engineering, with the identical methods used in order to simulate the OoP inertial forces; hence, such methods here are referred as *inertial*. Uniquely, the field of seismic engineering also developed additional methods of testing such structures; namely, dynamical and inter-storey drift methods. Dynamical methods are handled on shaking tables, while inter-storey drift methods load the frame rather than infill. Furthermore, many studies are intertwined between the blast and seismic engineering fields. For instance, Gabrielsen et al. (1975) from the blast engineering field cited arching-actions observed in 1967 Caracas and 1971 San Fernando earthquake.

In addition, there are other branches that study the same phenomena. However, they are not studied thoroughly as the main ones. They include effects of wind (Anderson and Bright, 1976) load and soil pressure (Jäger et al., 2008). This paper presents the literature review of OoP and bidirectional behaviour of infilled frames in focus of seismic engineering.

Additionally, there are also various OoP experiments conducted on load-bearing brickwork (no frame) such as in Drysdale and Essawy (1988); Hallquist (1970); Lam et al. (2003); Vaculik (2012). Their findings have numerous similarities to inertial tests of infilled frames. In this paper however, only few such studies are included as the main focus of this paper was on framed structures alike.

This paper is a literature review that included various journal and proceeding papers as well as thesis's (M. Sc. & Ph. D). The review scoped manuscripts published until the end of 2018's.

Furthermore, for a state-of-the art, systematic review that filters articles from specific electronic indexing bases, readers are encouraged to read the paper under reference Furtado et al. (2018b). Also, if one is interested in further information about analytical models, authors recommend an article that investigates their reliability Pasca et al. (2017). For overall review of literature that also includes macro- and micro-models, please remark reference Asteris et al. (2017).



(a) Parapet wall inertial failure, Kaikoura earthquake (EERI, 2018)



(b) Façade masonry wall inertial failure, Kaikoura earthquake (EERI, 2018)



(c) Muisne earthquake inter-storey drift failure, Ecuador (EERI, 2018)



(d) Muisne earthquake inter-storey drift failure, Ecuador (EERI, 2018)



(e) Muisne earthquake inter-storey drift failure, Ecuador (EERI, 2018)



(f) Muisne earthquake mix of inter-storey drift and inertial failure, Ecuador (EERI, 2018)

Figure 2: Various failures as recorded after real earthquake scenarios

2 Review of experimental campaigns

This section covers a review of experimental assessments of infilled frames in regards to OoP and bidirectional loading within the scope of seismic engineering. Data from experimental campaigns was gathered and presented in Tables 2, 3, 4 & 5. The distribution of various characteristics from Tables 2 - 4 are plotted on Figures 5 - 7, and of Table 5 on Figure 21. From provided tables, it is clear that frames are

made as strong or weak, constructed either of RC or SS. Infill panels were built; mostly, as a single leafed vertically laid clay or concrete blocks or bricks. There are exceptions, mainly in Portuguese research, where traditionally, blocks are laid horizontally. Portuguese masonry also possesses lower compressional strength (Tab. 5), likely due to the direction of voids. Various conditions were tested in order to examine their influence on OoP behaviour, such as: boundary conditions; slenderness; aspect ratio; effects of gravity load and etc.

Furthermore, one can point out that most experiments were conducted with inertial methods. Mostly with a single-leaf air-bags, loaded in one direction (Tab. 2, Fig. 4c). The cyclic, quasi-static air-bag OoP loading method is conducted in one direction by loading and unloading the infill, i.e. by pressuring and unpressurising the air-bag.

Less studies were done on shaking tables, where the excitation was provided by an earthquake signal or a sine wave (Tab. 2, Fig. 4d). Also, there are only two authors (Henderson et al., 1993; Flanagan and Bennett, 1999b) that researched the inter-storey drift method. Mainly as a counter part of bidirectional studies (Tab. 2, Fig. 4d).

Most bidirectional tests were done firstly by implementing IP inter-storey drift force to the beam; after which, the infill was loaded inertially with OoP loads. Conjointly, there was only one experiment carried out to study the effects of previous OoP damage on IP behaviour, and only one with simultaneous OoP and IP loading. Both of those studies were carried out by Flanagan (1994).

Furthermore, researchers did recognize the importance of connection between frame and infill, i.e. boundary conditions which many of them studied. Some researchers as Akhoundi et al. (2016) refer to boundary conditions as effects of workmanship, as building in-site can result in loss of connections due to poor workmanship. Most commonly, the effects of poor workmanship is reflected through partial or absent connection between the upper beam and infill (Fig. 9b). As that connection is harder to fill. Others, such as Wilton and Gabrielsen (1973) refer to gaps as “practical consideration”, since infill can move more or less independently from the frame. Such considerations were done by disconnecting the columns from infill (Fig. 9c). Correspondingly, Fowler (1994); Tu et al. (2010) found in dynamic and Flanagan and Bennett (1999b) in OoP inter-storey drift cyclic test; that infill and frame move together as a single unit. Thus, a disconnection can cause an independent action between the two; and with it, magnify the infill’s inertial forces. Ergo, due to loss in connection, inertial failure can occur as it was the case with A1 specimen (Fig. 20a) of Tu et al. (2010).

Research also focused on openings. Namely, with the IP studies it was shown that openings reduce bearing capacity and affect failure mechanisms (Sigmund and Penava, 2014; Surendran and Kaushik, 2012; Tasnimi and Mohebkah, 2011). However, the same can not be stated with certainty, as there were some opposing results in OoP studies. Furthermore, Figure 3 shows all openings that were studied in the field on OoP loading of infilled frames. Presumably similar window opening as in Figure 3a has been tested by Dawe and Seah (1989); however, figures and detailed descriptions are missing. By the same reason, a presumably similar full height opening as in Figure 3e was tested by Verlato et al. (2016). It is to be noted that all openings were placed centrally and all were tested with inertial methods. Also, their area to infill’s ratio is $A_o/A_i > 10$. Hence, it is within a limit by which opening size plays a role in masonry behaviour as stated by EN1996-1 provisions (BSI, 2004). Figure 6c was not made as a box plot because there were only 6 data points. On the same Figure 6c a BSI (2004) limit was plotted. Namely, it states that openings with the ratio of $A_o/A_{in} \leq 10$ can be neglected.

Studies that included effects of gravity load were those of Rabinovitch and Madah (2011); Furtado et al. (2018a); Klingner et al. (1996); Fowler (1994). Hence, the majority were done without.

2.1 Arching action & boundary conditions

The principal finding of the field was that, unlike the expected flexural induced failure; a compressive, arching-action failure occurs. This was first discovered on URM wall tests by the Armour Research Foundation in 1951 (McDowell et al., 1956b). From there, McDowell in 1956 (McDowell et al., 1956b) under the US Air Force opened a discussion about the newly found arching-action. He hypothesised about a solution to the question as why do masonry walls obtain six times greater resistance than simply supported slabs. He argued that it was due to additional compressive forces developed by arching-action. The hypothesis was approved; and today, arching-action is a standard phenomena of the field and it transited into a theory, termed *arching-action theory*. McDowell et al. (1956a) was also the first to develop equation with which one can calculate the ultimate OoP resistance of load-bearing brickwork with the effect of arching-action (Eq. 2).

Table 2: OoP experimental loading methods and boundary conditions

#	Study by	OoP load type	OoP loading method	IP loading method	Gaps considered		
					None	@ beam	@ columns
1	Dawe and Seah (1989)	Monotonic	Inertial - AB	No	+	+	+
2	Henderson et al. (1993)	Cyclic	Inter-storey drift	Cyclic	+	-	-
3	Angel et al. (1994)	Monotonic	Inertial - AB	Cyclic	+	-	-
4	Fowler (1994)	Dynamic	Shaking table	Dynamic	+	-	-
5	Klingner et al. (1996)	Dynamic	Shaking table	Dynamic	+	-	-
6	Flanagan and Bennett (1999a)	Monotonic & Dynamic	Inertial - AB & inter-storey drift	Cyclic	+	-	-
7	Hashemi and Mosalam (2007)	Dynamic	Shaking table	No	+	-	-
8	Tu et al. (2010)	Dynamic	Shaking table	No	+	+	-
9	Komaraneni et al. (2011)	Dynamic	Shaking table	Cyclic	+	-	-
10	Liu et al. (2011)	Dynamic	Shaking table	No	+	+	-
11	Pereira et al. (2011)	Cyclic (q-static)	Inertial - double-leaf AB	Cyclic	-	+	-
12	Rabinovitch and Madah (2011)	Dynamic	Shaking table	No	+	-	-
13	da Porto et al. (2013)	Monotonic	Inertial - L	Cyclic	+	-	-
14	Hak et al. (2014)	Cyclic (q-static)	Inertial - P	Cyclic	+	-	-
15	Akhoundi et al. (2015, 2016)	Cyclic (q-static)	Inertial - AB	No	+	+	-
16	Furtado et al. (2015)	Cyclic (q-static)	Inertial - AB	Cyclic	+	-	-
17	Petrus et al. (2015)	Cyclic (q-static)	Inertial - L	No	+	-	-
18	Preti et al. (2015)	Cyclic (q-static)	Inertial - P load	Cyclic	+	+	-
19	Misir et al. (2016)	Cyclic	Inertial - AB	Cyclic	+	-	-
20	Mosoarca et al. (2016)	Cyclic (q-static)	Inertial - L	No	+	-	-
21	Verlato et al. (2016)	Monotonic	Inertial - P load	Cyclic	+	-	-
22	Arède et al. (2017)	Cyclic (q-stat.) & monotonic	Inertial - AB	Cyclic	+	+	-
23	Sepasdar (2017)	Monotonic	Inertial - AB	No	+	-	-
24	Wang (2017)	Monotonic	Inertial - AB	No	-	+	+
25	Domenico et al. (2018)	Cyclic (q-static)	Inertial - P load	No	+	+	+
26	Rupakhety and Ólafsson (2018)	Cyclic (q-static)	Inertial - AB	Monotonic	+	-	-

AB - airbag, P - point, L - line

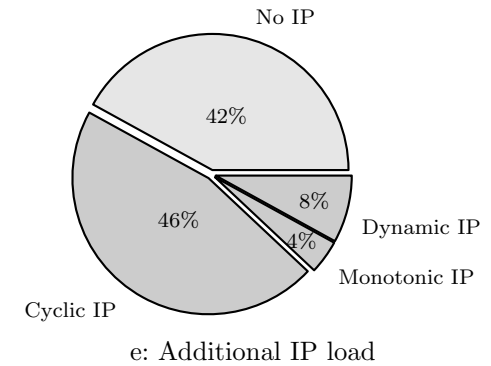
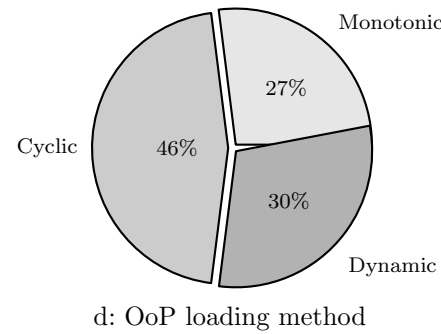
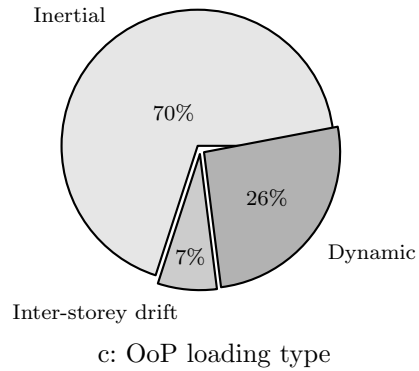


Figure 5: Distribution of OoP load methods

Table 3: OoP experimental tests material characteristics and subject studied

#	Study by	Frame	Infill	Subject studied
1	Dawe and Seah (1989)	SS	Concrete blocks dry and normally stacked blocks, boundary conditions	Effects of centric window opening (19%)
2	Henderson et al. (1993)	SS	Clay block layed horizontally	OoP+IP loading
3	Angel et al. (1994)	RC	Double leaf clay brick & concrete blocks	Infill slenderness variation h/t , variation of mortar type
4	Fowler (1994)	SS	Clay block	
5	Klingner et al. (1996)	RC	Clay brick	Weak and strong frames
6	Flanagan and Bennett (1999a)	SS	Clay block	IP+OoP & OoP+IP seperate and combined loading
7	Hashemi and Mosalam (2007)	RC	Hollow clay bricks	
8	Tu et al. (2010)	RC	Clay brick	Confined and un-confined panels
9	Komaraneni et al. (2011)	RC	Clay brick	Studied weak & strong frame with confined and unconfined infill
10	Liu et al. (2011)	RC	Concrete blocks	Special reinforced beam-infill connections observed
11	Pereira et al. (2011)	RC	Hollow clay brick	
12	Rabinovitch and Madah (2011)	RC	Concrete blocks	Gap between infill and columns
13	da Porto et al. (2013)	RC	Clay block	Study included URM & reinforced masonry units
14	Hak et al. (2014)	RC	Clay block	Full height centric opening (35%) and vertical stripes
15	Akhoundi et al. (2016, 2015)	RC	Hollow clay brick	Centric window opening (20%), Effect of contact surface between airbag & infill
16	Furtado et al. (2015)	RC	Single & double leaf hollow clay block layed horizontally	Effects of gravity loading
17	Petrus et al. (2015)	SS	Clay block	
18	Preti et al. (2015)	SS	Concrete block layed horizontally	Considered sliding joints to limit infill-frame response (from Preti et al. (2012))
19	Misir et al. (2016)	RC	Block: pumice, hollow-fired clay, autoclaved aerated concr. & Brick: insulated & horizontally hollowed clay brick with 13.5 cm thickness and horizontally hollowed clay brick with 8.5 cm thickness	
20	Mosoarca et al. (2016)	RC	Clay block	Inovative infill strengthening system
21	Verlato et al. (2016)	RC	Clay block	Inovative infill system <i>DRES</i> , centric full height opening (30%)
22	Arède et al. (2017)	RC	Clay block	Inovative test setup
23	Sepasdar (2017)	RC & SS	Concrete block	Considered centric window opening (17%)
24	Wang (2017)	RC	Concrete block	Considered centric door opening (17.6%)
25	Domenico et al. (2018)	RC	Clay block	Boundary variation study
26	Rupakhety and Ólafsson (2018)	RC	Clay block	Inovative earthquake-safe and eco-friendly infill panel systems

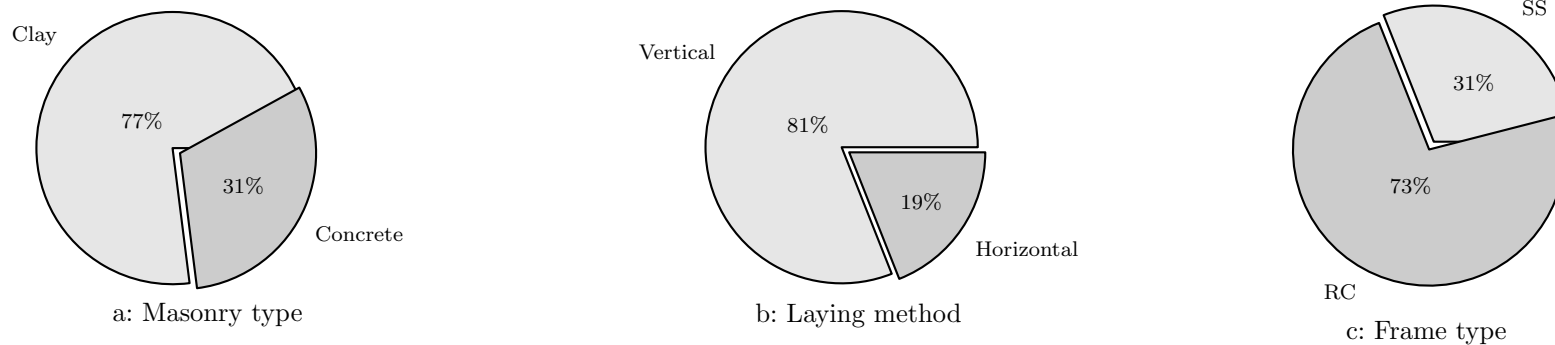
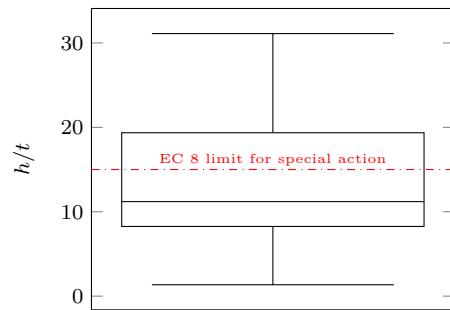


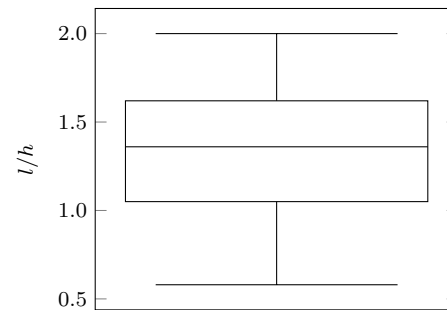
Figure 6: Material specifics of experimental tests

Table 4: OoP experimental tests geometrical characteristics

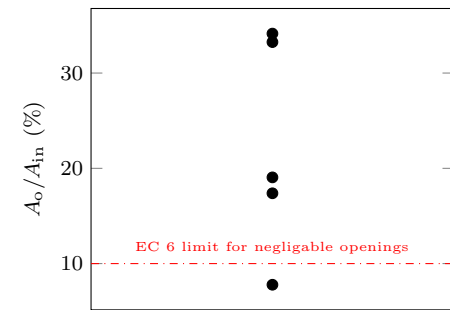
#	Study by	Infill			Openings		Scale	Specimens		
		h/t	l/h	A_o/A_{in} (%)	Type	#		Storeys	Bays	
1	Dawe and Seah (1989)	14.74, 20.00, 31.11	1.29	19.05	Window	1:1.0	9	1	1	
2	Henderson et al. (1993)	19.20	1.20			1:1.0	2	1	1	
3	Angel et al. (1994)	8.73, 39.68, 16.09, 10.73	0.75			1:1.0	8	1	1	
4	Fowler (1994)	10.12	1.64			1:1.0	1	1	1	
5	Klingner et al. (1996)	19.52	0.74			1:2.0	2	1	1	
6	Flanagan and Bennett (1999a)	22.40, 11.20, 6.79	1.00			1:1.0	3	1	1	
7	Hashemi and Mosalam (2007)	23.78	1.35			1:1.0	2	1	1	
8	Tu et al. (2010)	5.6	0.96			1:1.0	4	1	1	
9	Komaraneni et al. (2011)	22.67, 11.33	1.78			1:2.0	3	1	1	
10	Liu et al. (2011)	1.90	1.67			1:3.0	2	2	1	
11	Pereira et al. (2011)	2.33	2.00			1:1.5	4	1	1	
12	Rabinovitch and Madah (2011)	21.00	0.58			1:1.0	2	1	1	
13	da Porto et al. (2013)	22.08	1.57			1:1.0	6	1	1	
14	Hak et al. (2014)	12.55	1.43	34.14	Full wall height	1:1.0	5	1	1	
15	Akhoundi et al. (2016, 2015)	14.86	1.48	12.45	Window	1:2.0	6	1	1	
16	Furtado et al. (2015)	2.33, 1.35	1.29			1:1.0	3	1	1	
17	Petrus et al. (2015)	14.00	0.84			1:1.0	1	1	2	
18	Preti et al. (2015)	11.50	1.24	7.78	Window	1:1.0	2	1	1	
19	Misir et al. (2016)	8, 8.51, 10.53, 14.85, 23.53	1.80			1:1.0	6	1	1	
20	Mosoarca et al. (2016)	1.40	0.76			1:1.0	3	1	2	
21	Verlato et al. (2016)	9.17	1.40	33.25	Full wall height	1:1.0	4	1	1	
22	Arêde et al. (2017)	1.53	1.83			1:1.0	5	1	1	
23	Sepasdar (2017)	10.89	1.37	17.38	Window	1:2.0	4	1	1	
24	Wang (2017)	10.89	1.37	17.38	Door	1:2.0	4	1	1	
25	Domenico et al. (2018)	29.38	1.28			2:3.0	3	1	1	
26	Rupakhety and Ólafsson (2018)	7.60	1.84			1:1.0	7	1	1	



a: Distribution of slenderness (h/t)



b: Distribution of aspect ratio (l/h)



c: Distribution of A_o/A_{in} ratio

Figure 7: Distribution of geometrical characteristics

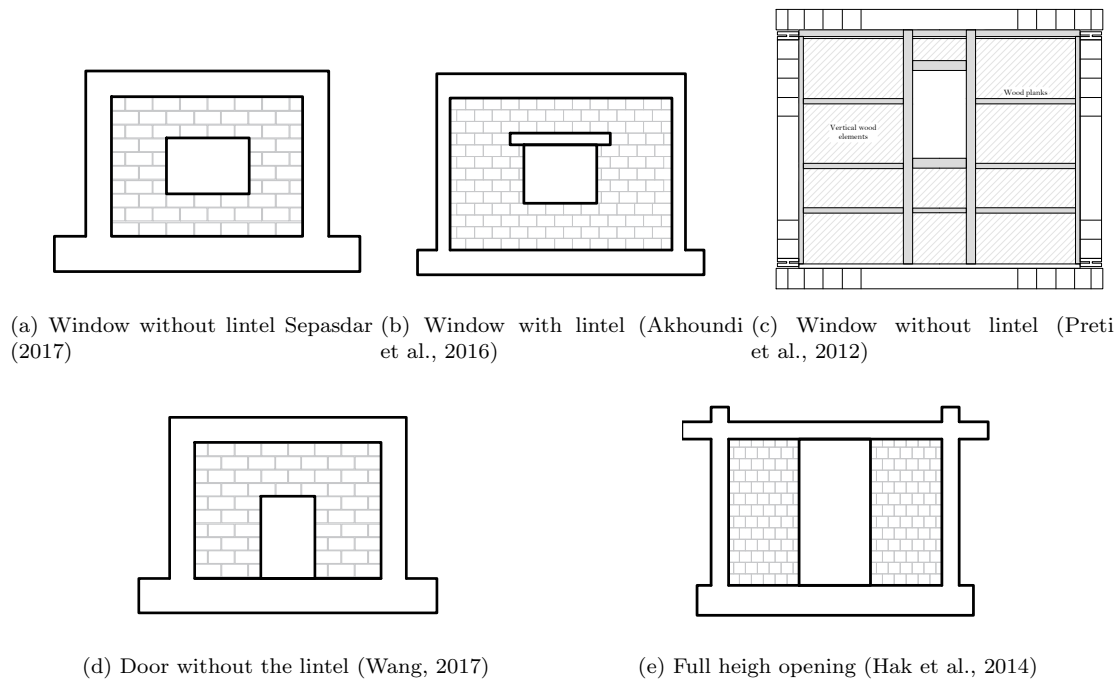


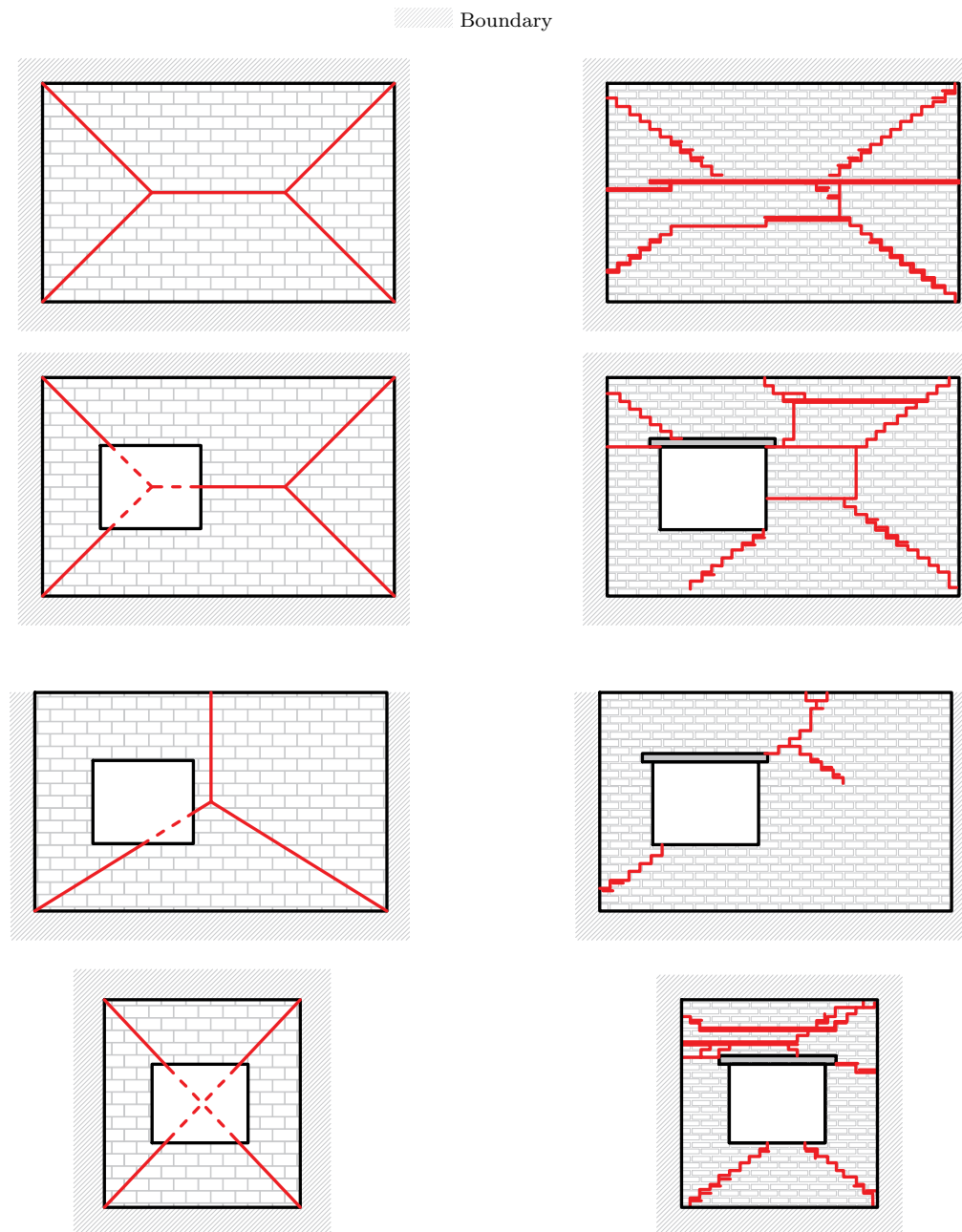
Figure 3: Opening considered in OoP research

The development of arching-action (Fig. 8a) as described by Moghaddam and Goudarzi (2010); Dawe and Seah (1989), starts with the bending of infill. Infill bends as a flexible beam would, until it cracks. Most commonly at three points: 1. Interface – Mid-height; 2. & 3. Boundary cracking (crushing at the frame). Those three points on one end clamp and on the other, open. Clamping points create the compression arch or compressive membrane forces (Flanagan and Bennett, 1999a) (Fig. 10a) that resist transversal ones. Such arching action was firstly refereed by McDowell et al. (1956b) as a *three-hinged arching-action* after similar bearing mechanism of a three hinged arch. Furthermore, diagonal cracks start to propagate from the upper half of the infill until they meet with horizontal cracks at the mid points. From there, diagonal cracks start to progress on the lower half of the infill. The yielding pattern is similar to those in plate theories (Quintas, 2003).

Moghaddam and Goudarzi (2010) found that high slenderness, low boundary stiffness or weak infill material may cease arching-action development or its benefits may be limited. Correspondingly, Moghaddam and Goudarzi (2010) divided the problem in two modes: 1. Crushing at the boundary and 2. Transverse instability. Crushing at the boundary occurs when thick panels are crushed at the supports (frame), while transverse instability failure, from excessive transversal deflections. The transverse instability is the favourable mode as the benefits of arching-action are thus magnified. The same analogy can be drawn from the plate and shell theory, whereas panels with low slenderness, their behaviour may be less influenced by membrane forces as is it the case for thick plates and shells (Flanagan and Bennett, 1999a).

Boundary conditions affect failure modes (Fig. 9), load-bearing and deformation capacities (Fig. 11) and arching-action mechanism (Fig. 10). If the infill is bounded by all sides, two-way action (horizontal and vertical arching) occurs (Fig. 9a & 10a) and with it, greater load-bearing & deformations capabilities (Fig. 11). Yet, if infill is bounded by three (infill-beam gap) or two sides (infill-columns or infill-beams gap) one-way action occurs (Fig. 9b & 9c). Then, load-bearing and deformation capabilities are lowered in comparison to fully bounded ones (Fig. 11). Single gapped, one-way arching-action (Fig. 9b) has both vertical and horizontal aching. However, the horizontal arch is a three-hinged (Fig. 10f); hence, less effective. While in two-way horizontal arching action it is the four-hinged arching-action (Fig. 10e). Comparatively, the double gapped is a truly one-way arching-action (Fig. 9c) as it has only vertical or horizontal, three-hinged arching action. Hence, lowest OoP resistance.

Figures 11 & 14b lead to the conclusion that the less connection between the infill and frame there is, the greater loss in load-bearing and deformation capabilities. The force-displacement curves from Dawe and Seah (1989) show greater differences in initial stiffness, and less effect on deformation capabilities between various boundary conditions. However, results from Akhoundi et al. (2016) and Domenico et al. (2018) show less profound change in initial stiffness and in load-bearing outcomes (Fig. 11). Yet, both graphs show great reduction of deformation capabilities. The differences can be attributed to the spe-



(a) Mays et al. (1998) failure assumption of walls with window opening failures (b) Griffith et al. (2007) experimental results of walls with window openings

Figure 4: Mays et al. (1998) prediction of failures vs. Griffith et al. (2007) experimental outcome of load-bearing walls

imens slenderness. Dawe and Seah (1989) have profoundly thicker panels when compared to those of Domenico et al. (2018) (Tab. 4). Additionally, note that specimens containing infill-columns interface gaps had very brittle behaviour due to crushing soon after reaching peak load (Fig. 11).

The symmetrical, two-way arching-action is sometimes referred to as rigid-arching-action (Fig. 10) and unsymmetrical one-way, so called gapped-arching-action (Gabrielsen et al., 1975). As explained by Wilton and Gabrielsen (1973), when a gapped panel is loaded, infill bends as a cantilever would until it reaches the frame. Then, infill cracks at the bottom and wedges. After cracking, the divided elements develop the compression arch (Fig. 8b). However, arch has a linear (thrust) part on the upper and non-linear (arch) on the lower half of the infill.

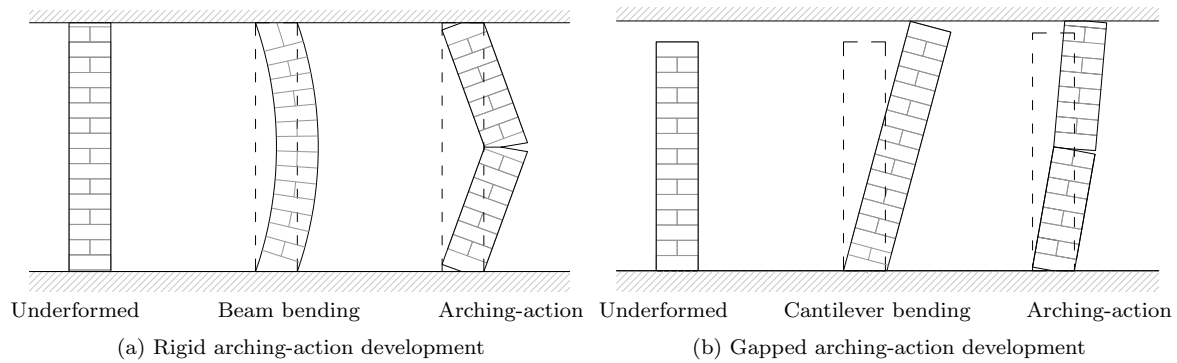


Figure 8: Arching-action development phases by different boundary conditions

Additional vertical arching-action modes were found; however, they not as common as three-hinged action. They include two- and four-hinged arching-action. The two-hinged arching-action (Fig. 10c) was observed on dynamical tests carried out by Tu et al. (2010). The two-hinged arching-action starts by infill's cracking on the tension sides of the panel (top and base), thus a diagonal thrust forms (not arch) between the opposite compression sides. Then, the panel segment rigidly rocks between the crushed ends. Tu et al. (2010) concluded that such behaviour is analogous to a slender rocking pier. The two-hinged arching action is in an essence a compression strut; however, for the sake of uniformity, it will be refereed as an arch. It is to be noted that two-hinged arching-action is the only instance of specifying arching-action in dynamical experiments. Four-hinged, vertical arching-action (Fig. 10d) was found by Varela-Rivera et al. (2012) on confined masonry panels. Such arching action can be expected with high walls, and the product of rigid, horizontal arching-action (Fig. 10e).

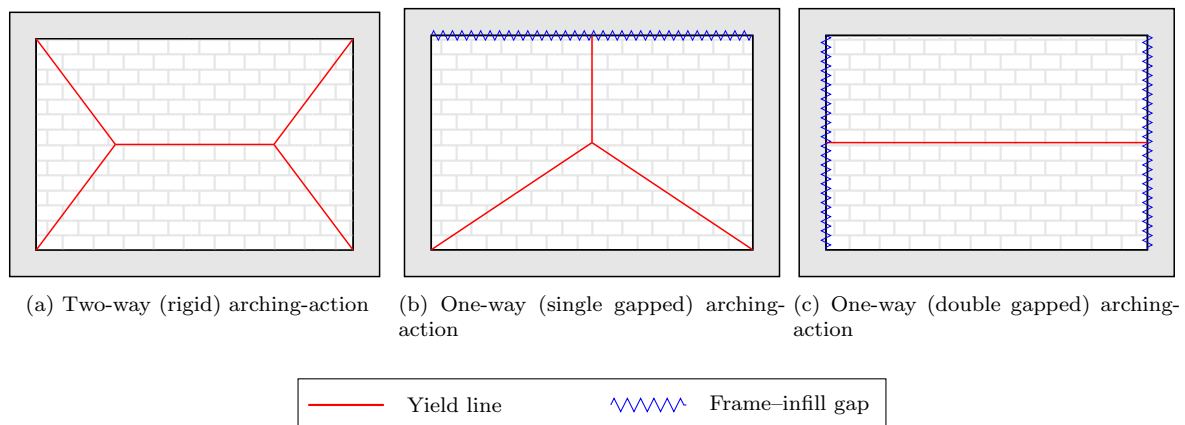


Figure 9: Types of arching-action in relation with boundary conditions

2.2 Effects of openings

All experimental efforts of addressing the effects of openings were done using inertial methods with centrally positioned openings. Window opening of Preti et al. (2012) (Fig. 3c) was not scoped within this paper because of its specific infill assemblage and the fact that it falls in the area of negligence ($A_o/A_i \approx 8 < 10\%$) by EN 1996-1-1 provisions (BSI, 2004). Other openings had their area in range of $A_o/A_i \in [17, 30] > 10\%$ when compared to the area of infill. Hence, they exceeded the limit of negligence.

It was found that all openings cause significant reduction of deformation capabilities when compared to fully infilled frames (Fig. 14). Yet, same was not evident in regards to load-bearing capacities, as different authors had different outcomes. For instance, Akhoundi et al. (2016) and Dawe and Seah (1989) found no reduction of bearing capacities; while, (Wang, 2017; Sepasdar, 2017; Verlato et al., 2016) observed a significant decrease. To reflect the area of openings to difference in ultimate force and displacement Figure 14d was produced. Note that the pure OoP loading from Verlato et al. (2016) containing an opening was

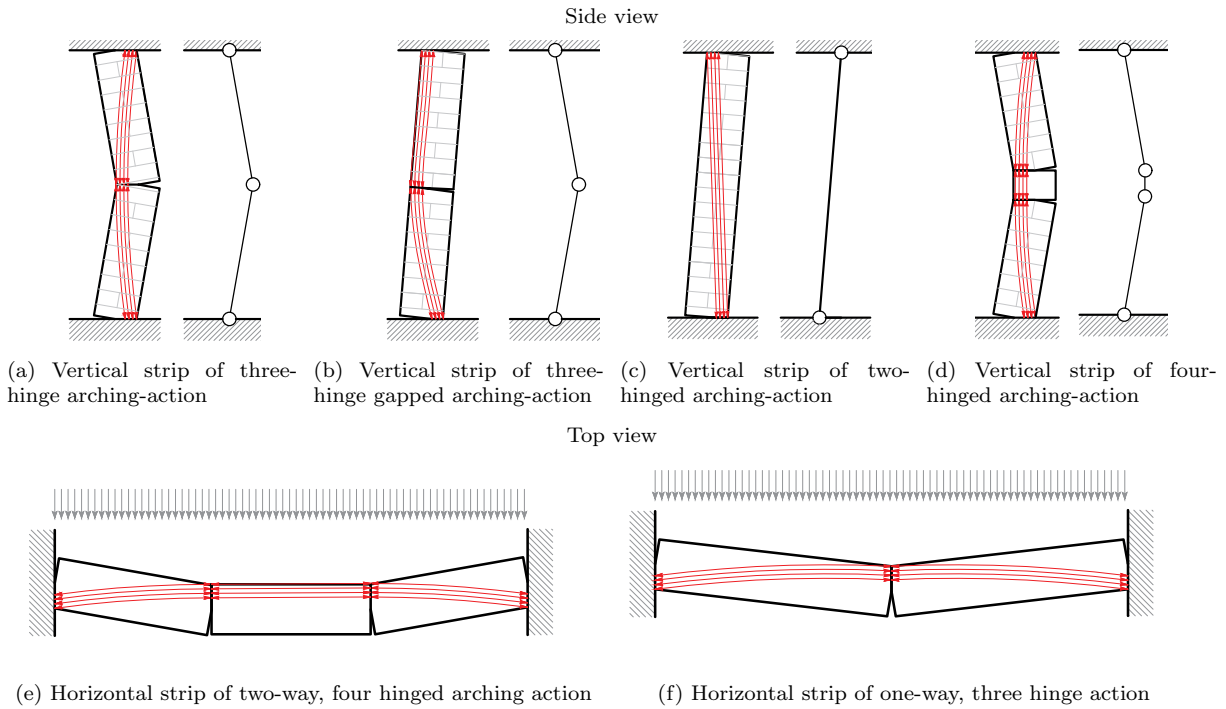


Figure 10: Observed arching-action modes with their equivalent models

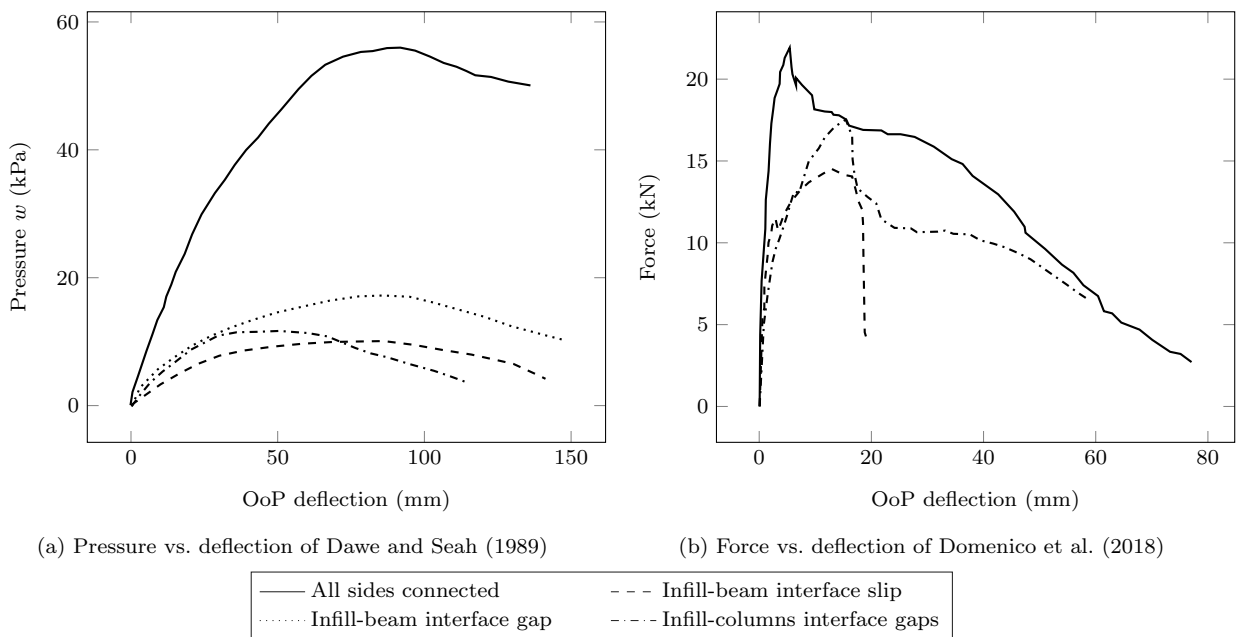


Figure 11: Force – displacement curves of various boundary condition

compared with the full infill that had previous 2.5% IP inter-storey drift i.e. previous IP damage. By the same figure, no logical conclusion about the impact of opening size can be drawn. Contrariwise, Mays et al. (1998) in blast engineering studies of RC panels with openings proposed a linear degradation of window and increase of doors ultimate resistance in relation to opening area. The reduction of door and window openings as noted in Figure 14d were derived from Equation 16 and Table 8 (Mays et al., 1998) as $F_r(A_o/A_i)$.

By observing crack patterns of infills with openings (Fig. 13), along with load-bearing graphs, it is evident that arching-action was able to develop. It is above all, clear in the case of window openings (Fig. 13b, 13c) as familiar rigid arching-action “X” pattern emerges (Fig. 10e). Also, it is evident that opening type does influence the arching-action. Particularly, window had greater capabilities of forming

arching-action than door or full height openings. Openings had a slight impact on initial stiffness (Fig. 14d); whereas, door had more influence to initial stiffness than the window opening (Fig. 14a).

Results of full height opening by Hak et al. (2014) are not published in cited paper nor other. In studies by Dawe and Seah (1989) detailed descriptions, ultimate displacement value, force-displacement graph nor crack patterns were found for the specimen with window opening. Also, Verlato et al. (2016) crack patterns of the specimen with full height opening is unavailable. Ergo, there is no data available about full height opening crack patterns.

The copious difference in resistance reduction between Akhoundi et al. (2016); Dawe and Seah (1989) (Fig. 13c) and Sepasdar (2017) centric window (Fig. 13b, & 14d) tests may be due to lintel. Window with lintel obtained resistance almost the same as fully infilled one. Moreover, yielding lines did develop at the lower half of the infill. Same can not be observed for the specimen without lintel. Likewise, in preliminary studies by Anić et al. (2018), lintel has accumulated greater amounts of compressive stress; hence, additional clamping point in the arching-action curve.

It is noticeable that crack patterns of specimen with door opening (Fig. 13a) do not resemble the arching-action patterns as window openings do. All cracks are more or less vertical. Similar patterns are obtained on OoP tests of load-bearing RC walls (without frame) with eccentric door opening by Mays et al. (1998) (Fig. 12b). Door opening from Mays et al. (1998) (Fig. 12b) some-what resemble the double gapped yield line (Fig. 9c). This can be explained as the first crack separates right and left side of the wall (Fig. 12b), thus, changes to boundary condition. New boundary conditions are similar to those of the double gapped condition (Fig. 9c).

Mays et al. (1998) also tested a specimen with both door and window opening. There, similar results were obtained. Firstly, the crack separates left and right side, as it is done with eccentric door (Fig. 12b). The wall section between window and door acts as double gapped wall and cracks with a straight line in the middle. Other parts developed diagonal cracks. From a different point of view; firstly, door separates left and right side, from there a single gapped arching-action occurs on the right side (perpendicular view).

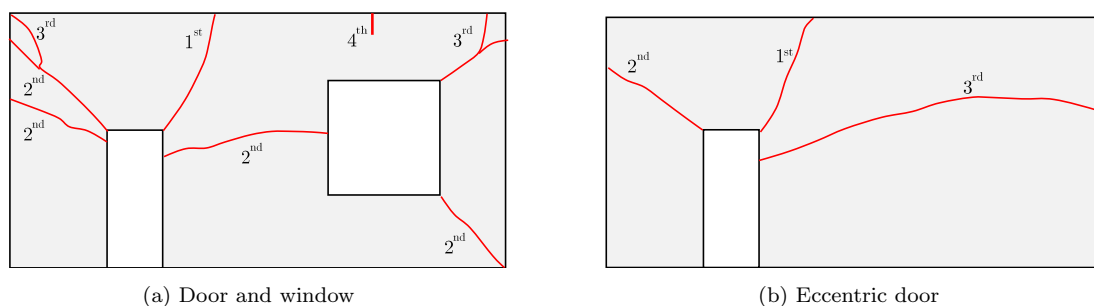
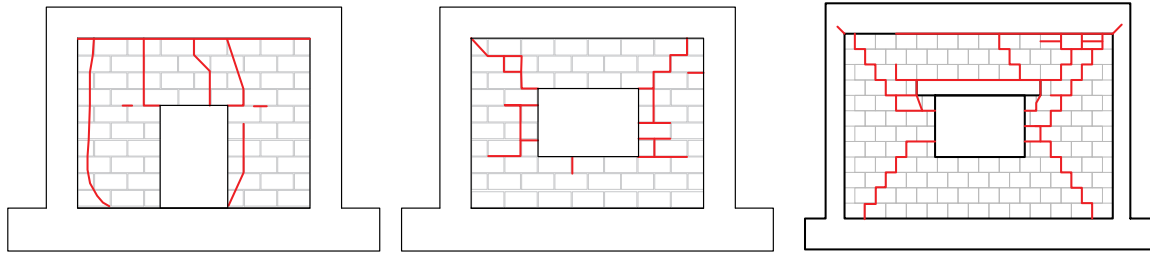


Figure 12: Results of Mays et al. (1998) URM wall test with designated crack occurrence

Load-bearing URM walls (without frame) with centric and eccentric window openings were tested by Griffith et al. (2007); Griffith and Vaculik (2007). In those studies rigid arching-action follows more or less the yielding line as it would without the openings. This is showed in Figure 4, where on the left side (Fig. 4a) is theoretical assumption by Mays et al. (1998) and on the right (Fig. 4b), tested URM walls by Griffith et al. (2007). It can be concluded that the prediction correlates highly with real crack patterns. However openings, especially their corners did influence the position and length of the yield lines. Nonetheless, the arching-action is evident. The specimen with aspect ratio of 1:1 had more horizontal than diagonal cracks.

Note that the original Figure 14a was in pressure w (kPa) vs. displacement; however, for comparison reasons, they were recalculated in forced F by the following equation 1.

$$F = w (A_{\text{infill}} - A_{\text{opening}}) \quad (1)$$



(a) Centric door opening by Wang (2017) (b) Centric window opening by Sepasdar (2017) (c) Centric window opening with RC lintel by Akhoundi et al. (2016)

Figure 13: Failure patterns of OoP specimens with openings

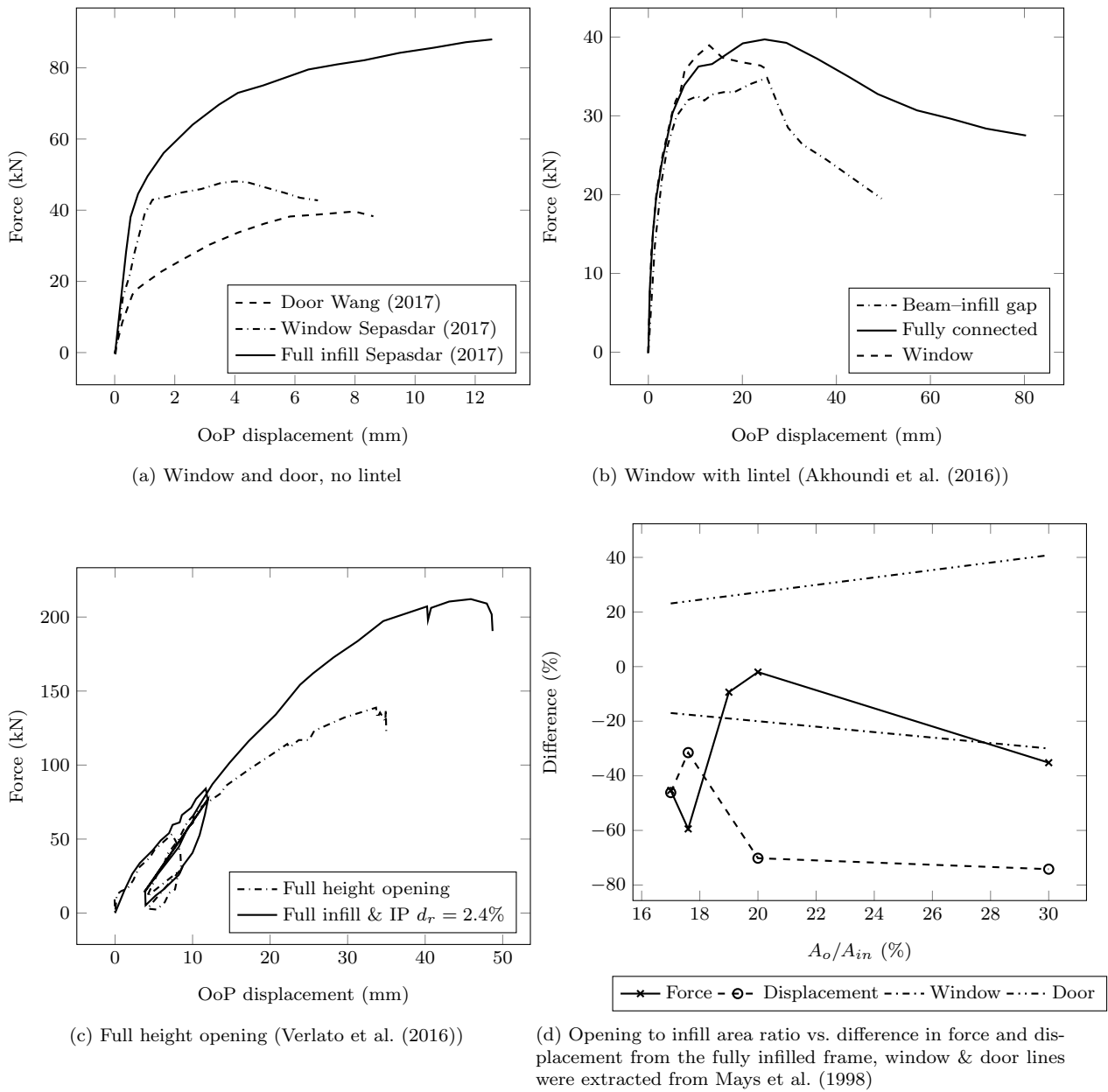


Figure 14: Force vs. displacement graphs of specimens with openings

2.3 Effects of slenderness & aspect ratio

Intuitively, due to compressive arching-action phenomena, slenderness and aspect ratio play a major roll on the OoP behaviour (Fig. 15). As stated in Section 2.1, slenderness may limit or bypass the arching-action (Moghaddam and Goudarzi, 2010; Dawe and Seah, 1989; Shapiro et al., 1994; Furtado et al., 2018a).

Figure 15 was derived from results published in Angel et al. (1994), where the change of load-bearing capacity was altered by different slenderness's. Curves were grouped by approximately similar masonry's compressive strength f_m , IP inter-storey drift d_r , same masonry unit and mortar type, while also including Eurocode 8 (BSI, 2005) limit of $h/t \leq 15$.

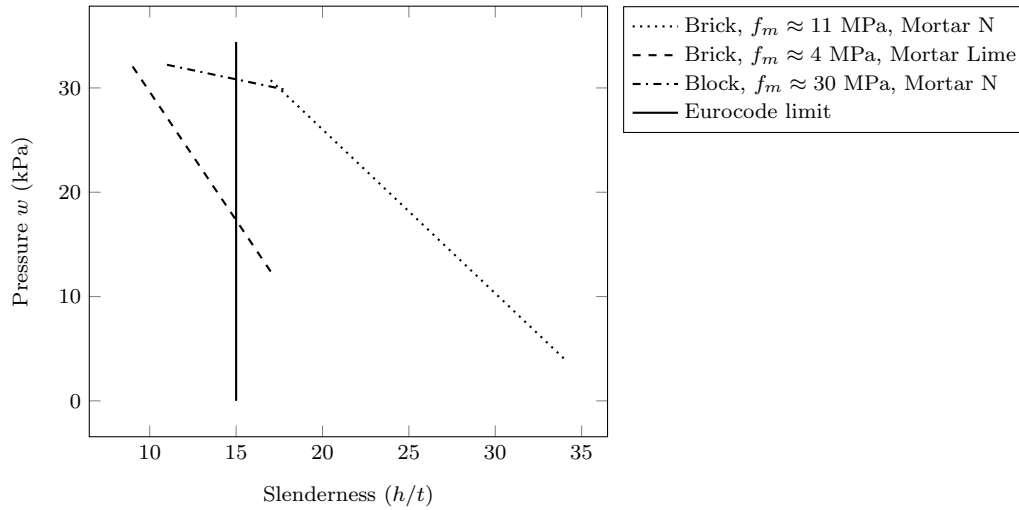


Figure 15: Effects of slenderness (derived from Angel et al. (1994))

Flanagan and Bennett (1999b) found that increase in walls thickness from 100 to 200 mm ($h/t : 22 \rightarrow 11$) resulted in three times greater ultimate force. In other words, doubling of infill's thickness tripled its OoP capacity.

By observing changes of aspect ratio in Figure 4, there is an obvious change of yield patterns. If the aspect ratio had greater values, horizontal line would develop at midpoints of diagonal lines. However, when the infill is square sized or at lower aspect ratio no horizontal line is developed, i.e. same as in plate theory.

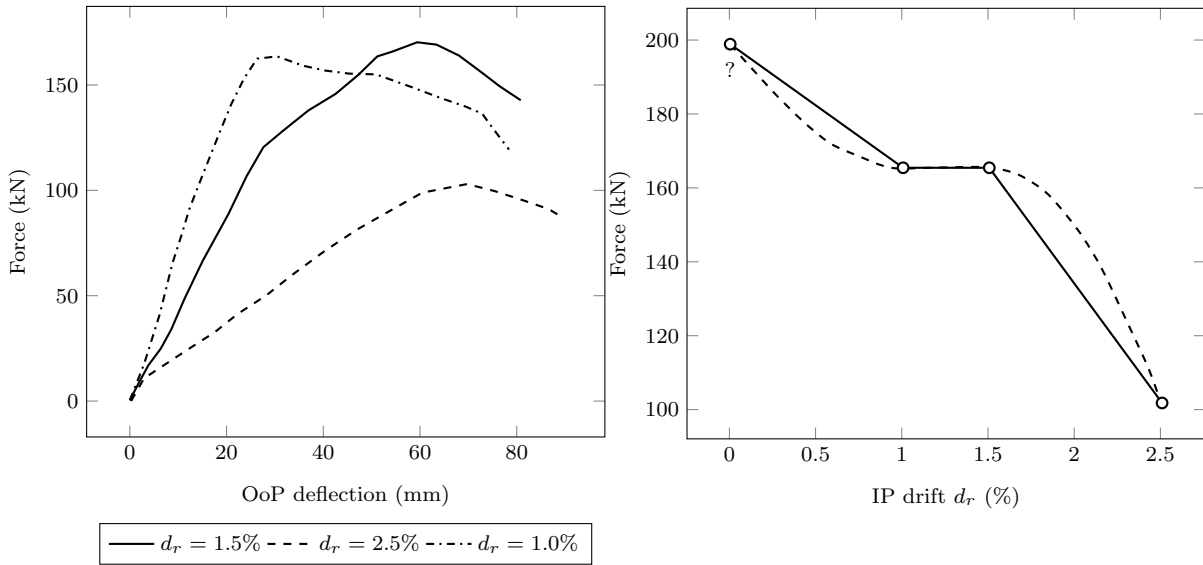
Furthermore, Komaraneni et al. (2011) found that specimens with slender walls experienced higher amplification of acceleration (inertial forces) with the maximum observed at mid-height. Yet, less slender specimen along the height acquired a nearly linear profile of acceleration response, however, with the maximum value near the top. Komaraneni et al. (2011) had a combination of inertial-dynamical test, i.e. where the frame was fixed from OoP translation and added additional masses to the URM panel.

2.4 Effects of bidirectional loadings

Nearly half of studies included previous IP test (Fig. 4e). Most researchers focused on prior IP damage. First such studies with infilled-frames were done by Angel et al. (1994), where it was concluded that previous IP damage could reduce OoP load-bearing capacity of slender panels for as much as one half. This was included in their equation, through R_1 factor (Eq. 5, Tab. 6). Similarly, Flanagan and Bennett (1999b) found that reduction can sum up to 15%.

Another study that focused in IP+OoP interaction was conducted by Hak et al. (2014) (Fig. 16). Results from different IP drift ratios is shown on Figure 16a. From there, one can conclude that previous IP damage decreases initial stiffness and ultimate force. Deformation capabilities were not greatly affected. Furthermore, Figure 16b was proposed by the authors to assess the degradation of OoP bearing capacity due to previous IP drift d_r . The question mark in Figure 16b points out that the point above is a conservative estimation by the authors. From there, one can mark that for each increase of $d_r = 1\%$ a average decrease of about 30% in OoP load-bearing capacity is implied. Hence, previous IP damage

drastically decreases OoP bearing capacity. Similar findings were also observed by Flanagan and Bennett (1999b); Angel et al. (1994); Dawe and Seah (1989).



(a) Force – displacement response for various IP drift ratios (b) Out-of-plane strength reduction in function of in-plane drift (Hak et al., 2014)

Figure 16: Effect of previous IP damage on OoP capacity (Hak et al., 2014)

Henderson et al. (1993) and Flanagan and Bennett (1999b) tested previous OoP inter-storey drift damage on IP’s load-bearing capacity (OoP+IP). Both concluded that prior inter-storey drift OoP damage had minimal effect to the overall IP performance especially to its capacity. This phenomena is certainly due to the fact that with inter-storey drift method, more damage occurs on the frame than on the infill. Namely, due to previous cracking of the infill, diagonal is weaker, i.e. softer, hence, initial stiffness is also lower when compared to the control IP groups. The corner crushing failure was not affected as observed by both research teams. Also, in the hysteric test by Henderson et al. (1993), the response is more linear than the IP hysteric curve. This strongly indicates that in the case of drift method there is less energy absorption when compared to IP tests.

Additionally, Flanagan and Bennett (1999b) had previous inertial OoP damage followed by IP loading, and simultaneous IP and inertial OoP (air-bag) loading. It was concluded that with inertial method the IP behaviour was profoundly affected, unlike with drift method. With combined IP+OoP (inertial) loading, Flanagan and Bennett (1999a) found a 40 % reduction of IP’s load-bearing capacity when compared with IP control specimen. Furthermore, simultaneous IP and OoP load Flanagan (1994) resulted in heavy damage, and yet, it remained stable. The unperceived stability was, presumably, the outcome of arching-action imposed by the air-bag.

2.5 Contrasting outcomes of different experimental methods

Benedetti and Benzoni (1984) stated that there are two forces acting upon a structures during ground motions: inertial and inter-storey drift. Also, Benedetti and Benzoni (1984) stated that inter-storey drift should cause more damage than the inertial forces (Benedetti and Benzoni, 1984).

Intuitively, dynamical - shaking table tests are the best experimental approaches for the field of seismic engineering. However, high costs and the demand for sophisticated equipment of such experiments, they are rarely used. Hence, many cyclic and static experiments are conducted instead.

Most experiments were done with inertial methods (Tab. 2), developed and also still used by the blast engineering field (Smith et al., 2016; Pereira et al., 2014). In those experiments, frame were fixed from OoP translations and infill was loaded. This can be questionable in the terms of seismic engineering, as during the ground motion, frames are excited not fixed.

On the shaking table tests by Fowler (1994) infill had similar or greater accelerations as did the frame (Fig. 18b). Moreover, the highest accelerations occurred on the top and 2/3 of the wall height

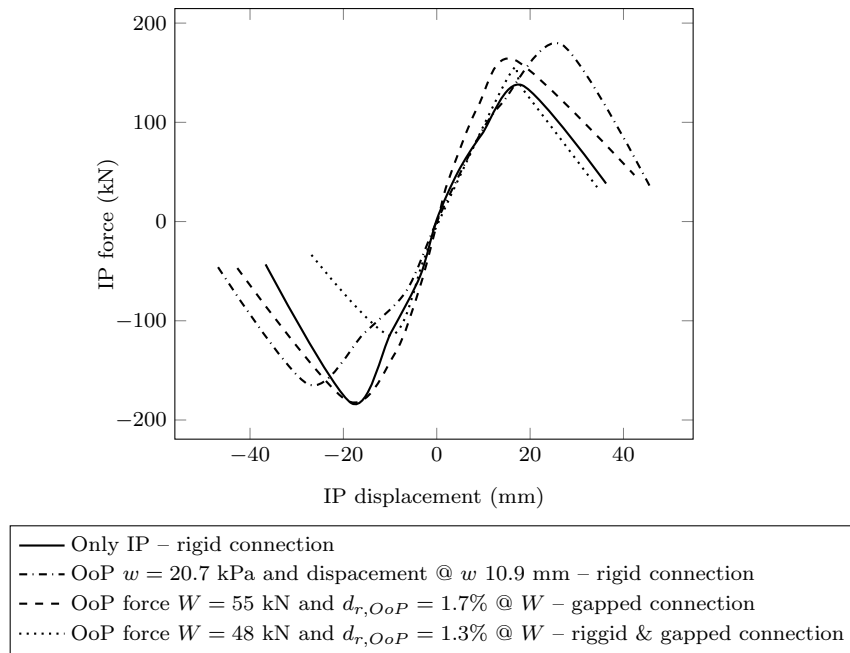
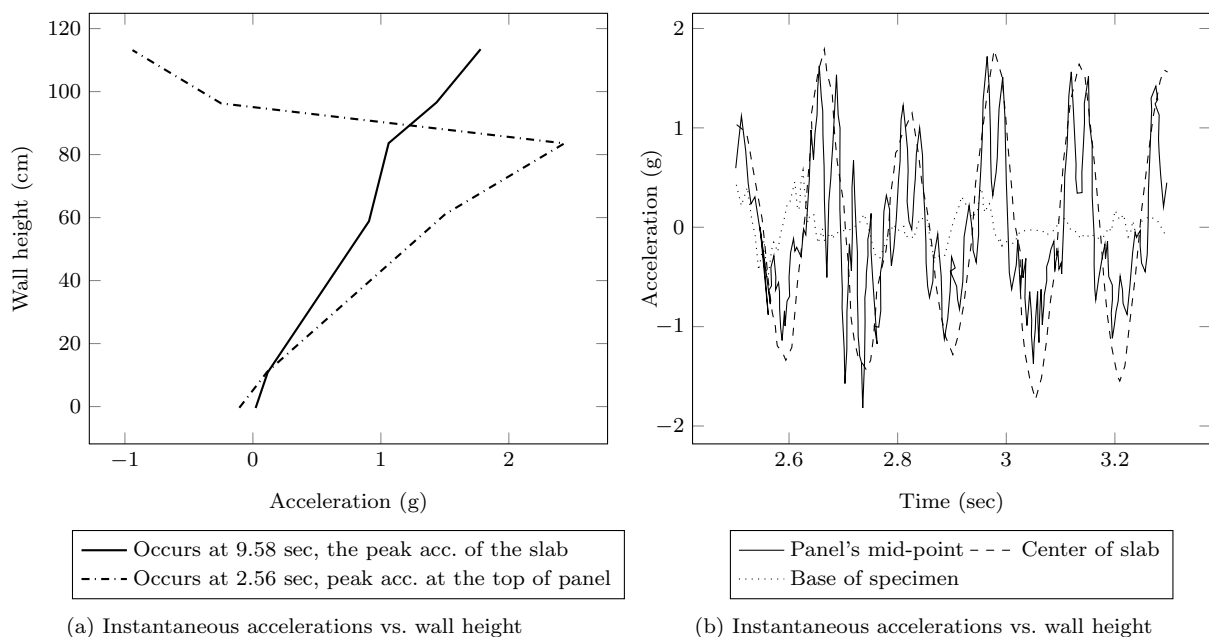


Figure 17: IP cyclic envelope derived from Flanagan and Bennett (1999b)

(Fig. 18a), similarly found by Tu et al. (2010). On one hand, Fowler (1994) and Tu et al. (2010) found in their dynamic and Flanagan and Bennett (1999a) in his inter-storey drift tests, that the frame and infill move together as a single unit. Which is not the case with inertial test. On the other hand, tests by Fowler (1994) showed largest displacements of the panel occurred at the infill's mid-point. In other words, the infill was affected more by the inertial forces. Furthermore, by examining damage states from the dynamical (Fowler, 1994; Tu et al., 2010) and inter-storey drift methods (Flanagan and Bennett, 1999b), it is clear that the frame sustained more damage than the infill. Also, Flanagan and Bennett (1999b) states that in his inter-storey drift test, frame failed, not the infill (Fig. 19). Henderson et al. (1993) also obtained more linear OoP response when compared to IP response. Hence, with OoP inter-storey drift forces, there is less energy absorption, i.e. infill's effects are not so pronounced.



(a) Instantaneous accelerations vs. wall height

(b) Instantaneous accelerations vs. wall height

Figure 18: Structure acceleration results from shaking table test by Fowler (1994)

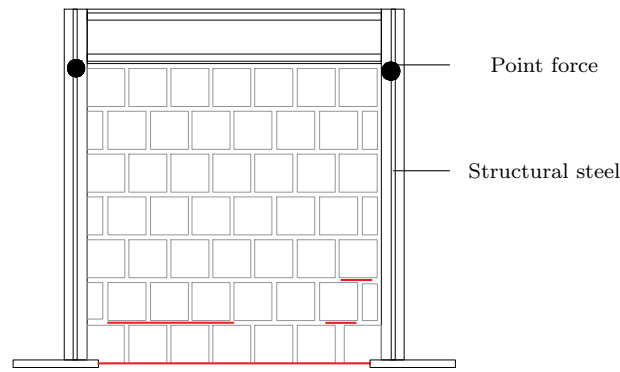


Figure 19: Crack patterns of inter-storey drift method (Flanagan, 1994)

Inertial methods are certainly great for load-bearing brickwork, parapet walls (Fig. 2a) and for framed masonry with a single or multiple gaps between the frame and infill. By disconnecting the frame from infill, they can act as separate elements. This statement goes in hand with the Wilton and Gabrielsen (1973) remark that by disconnecting the frame from infill one can act separately from the other. Thus, the greatly pronounced inertial characteristics of the infill can then cause the inertial collapse of itself. In other words, infill with a gap would be analogous to the parapet wall. The gap can be caused by workmanship or by IP loads. This was somewhat observed on one out of four specimens by Tu et al. (2010). A1 specimen lost a connection between the beam and the infill and as a consequence, it fell out due to inertia (Fig. 20a). In addition, inertial failures can be expected with very slender infills (Moghaddam and Goudarzi, 2010).

All three methods should be addressing the same phenomena, and yet, there are major differences between them. However, along with paper that computationally investigated inherent differences between the approaches (Anić et al., 2019) it was clear that there are more similarities between the dynamical and inter-storey drift methods. The greatest argument was that the frame is more damaged than the infill (Flanagan and Bennett, 1999b) (Compare Fig. 20b, 19 & 13), this is in direct contrast to the statement that frame does not play a role if it is purely loaded in OoP direction (Furtado et al., 2018b). This statement can also be reinterpreted that bare frames cannot be affected if loaded in OoP direction. Yet, in the research by Tu et al. (2010) bare frames also withstood great damages due to dynamical excitations. Various damages caused by the inter-storey drift forces were also observable in the real earthquake scenarios (Fig. 20), especially on walls that are orthogonal to those that suffered high IP damages (Fig. 2d). Inter-storey drift can also cause the beam to twist around its axis, and thrust the upper row of blocks (Penava and Sigmund, 2017). This also could lead to inertial failure due to loss of connection.

Regarding inertial methods, if the frame is discounted from the overall behaviour, the problem can be rendered as those of load-bearing brickwork. As in testing of such walls, frames can be included as to address walls boundary conditions.

2.6 Additional findings

Additional findings that are not discussed separately, but are nevertheless significant are listed below:

1. Mortar type does influence the OoP bearing with inertial methods Shapiro et al. (1994). Also, Shapiro et al. (1994) noted that lateral strength is directly proportional to compressive strength of mortar;
2. Two specimens from Flanagan and Bennett (1999b) had identical infill mechanical and geometrical properties but different frames. One is stronger (column $W410 \times 60$, beam $W460 \times 113$) and other is weaker (column $W250 \times 45$, beam $W310 \times 52$). The stronger frame developed 33 % greater ultimate force and 77 % greater displacement when compared with the weak frame. Hence, frame stiffness has great effects on OoP behaviour;
3. There was no significant difference between OoP behaviour of confined and unconfined masonry panels Tu et al. (2010);
4. Gravity load affects the OoP behaviour as it modified crack patterns and post peak behaviour as found by Furtado et al. (2018a). Contrariwise, in studies by Shapiro et al. (1994), it was found that gravity load does not affect the OoP behaviour.

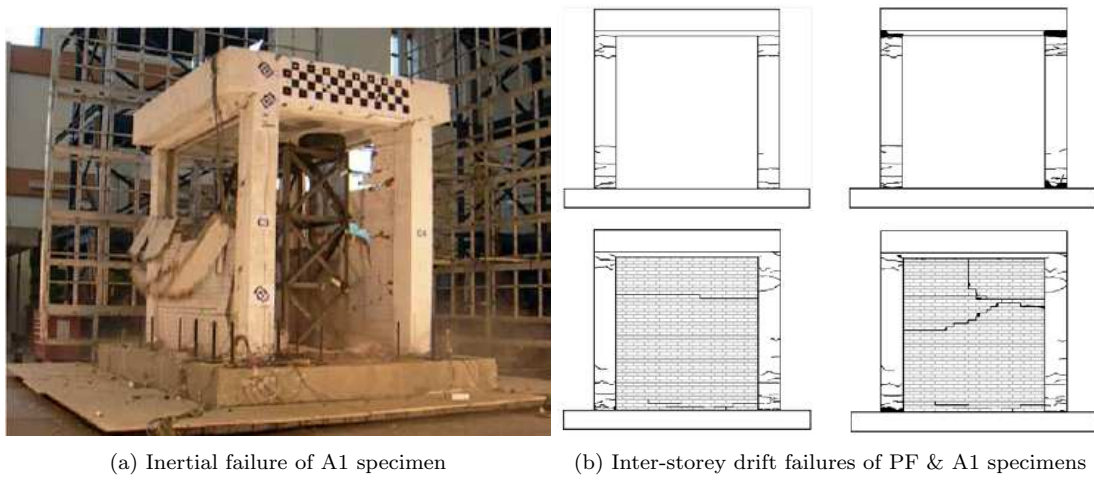


Figure 20: Damage states of various specimens of (Tu et al., 2010)

3 Analytical models

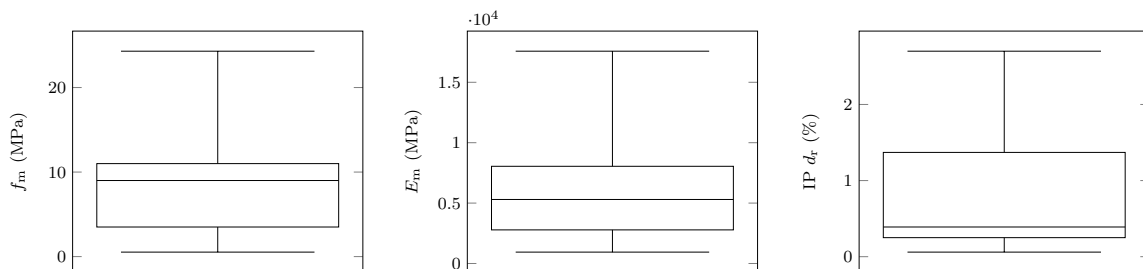
In this section, a study of analytical models is presented. The study included a comparison of analytical and experimental approaches; also, single and multi-variable parametric/sensitivity analysis of the analytical models. The aim of the parametric analysis was to gain insight in stability, reliability, models limitations and governing factors. Furthermore, the study was pinpointed on arching-action theory based models. Hence, flexural-action based as those from Drysdale and Essawy (1988); Haseltine (1976); Hendry (1973) were discarded. For more information about the flexural-action models, please refer to paper: Asteris et al. (2017).

At first, calculation of OoP load-bearing capacities were based on flexural-action theory. However, those were inadequate, as they provided capacities lowered up to six times than those observed in the experimental tests (McDowell et al., 1956b). As specified in Section 2.1, first arching-action based equation (Eq. 2) was developed by the same research team that introduced the concept of arching-action McDowell et al. (1956a). However, it was developed for the calculation of load-bearing URM walls (no frame) capacity. From that point, others followed the similar pattern of equation developing.

All current equations that were developed for the load-bearing estimation of infilled frames OoP are displayed in Table 6. Those equations (Eq. 5–6) were developed to interpret the effects of inertial forces. Correspondingly, there were no equations developed for inter-storey drift nor dynamical methods. Also, all equations were developed on the basis of vertical three-hinged arching-action.

$$w = \gamma \frac{f_m}{2(h/t)^2} \quad (2)$$

Where γ depends on h/t ratio.



(a) Distribution of masonry's compressive strength (b) Distribution of masonry's elastic modulus (c) Distribution of previous IP inter-storey drift

Figure 21: Distribution of mechanical properties from Tab. 5

Table 5: Various geometrical and mechanical properties of specimens

Author	Specimen	t (mm)	l (mm)	h (mm)	Frame type	Column size (mm×mm)	Beam size (mm×mm)	f_m (MPa)	E_m (MPa)	E_F (MPa)	Capacity w (kPa)	Displacement (mm)	Remark
Dawe and Seah (1989)	WE1	190									22.30	n/a	Trust type joint reinforcement
	WE2	190									19.20	n/a	Plain masonry panel
	WE3	190									7.80	n/a	dry-stack panel
	WE4	140									11.20	n/a	Plain masonry panel
	WE5	90	3600	2800	SS	W250 × 58	W200 × 46	24.3	17575	210000*	7.80	n/a	Plain masonry panel
	WE6	190									10.60	n/a	Plain masonry panel
	WE7	190									14.70	n/a	Truss type joint reinforcement
	WE8	140									13.40	n/a	Restraints against slipping
	WE9	190									17.40	n/a	Window opening
Angel et al. (1994)	1	48						11.50	8046		8.19	n/a	Pure OoP, S mortar
	2	48						10.81	8046		4.02	n/a	IP (0.34% d_r) + OoP, N mortar
	3	48						10.14	5212		5.99	n/a	IP (0.22% d_r) + OoP, Lime mortar
	4	92						22.90	12438		29.78	n/a	IP (0.09% d_r) + OoP, N mortar
	5	143	2740	1630	RC	305×305	203×254	21.46	11624	24821	32.22	n/a	IP (0.06% d_r) + OoP, N mortar
	6	98						4.59	2137		12.40	n/a	IP (0.25% d_r) + OoP, Lime mortar
	7	98						11.00	2923		30.74	n/a	IP (0.25% d_r) + OoP, N mortar
	8	187						3.50	2358		32.08	n/a	IP (0.39% d_r) + OoP, Lime mortar
Flanagan and Bennett (1999b)	25	100				W250 × 45	W310 × 52				8.10	25.30	Plain masonry panel
	18	200				W250 × 45	W310 × 52	5.60	5300		26.60	11.50	Plain masonry panel
	19	200	2240	2240	SS	W250 × 45	W310 × 52			199948	21.70	19.30	IP (0.8% d_r) +OoP
	22	330				W410 × 60	W460 × 113	2.29	5040		39.50	49.50	Plain masonry panel
Hak et al. (2014)	TA1										13.25	n/a	IP (1.50% d_r) + OoP
	TA2	235	4220	2950	RC	350×350	350×350	4.64	5299	32000*	8.11	n/a	IP (2.00% d_r) + OoP
	TA3										13.01	n/a	IP (1.00% d_r) + OoP
Akhoundi et al. (2015)	SIF-A										8.86	25.00	Beam - infill gap
	SIF-B	110	2415	1635	RC	160×160	270×160	1.00	1000*	32000*	10.13	12.00	Plain masonry panel
	PIF-A										9.88	25.00	Window opening
Furtado et al. (2015)	inf.01										7.76	22.00	OoP monotonic + gravity load
	inf.02	150	4200	2300	RC	300×300	300×500	0.53	941.9	24300	7.25	12.00	OoP cyclic
	inf.03	150+110									1.76	1.50	OoP cyclic + IP (0.5% d_r), 2 leafed
Sepasdar (2017)	IF-W										43.70	4.30	Window opening
	IF-ND	90	1350	980	RC	180×180	180×180	9.00	7650	16911	66.30	12.50	Plain masonry panel
	IF-D1										44.40	6.60	IP (0.66% d_r) + OoP
	IF-D2										26.40	9.90	IP (2.70% d_r) + OoP
Wang (2017)	IF-RC-DO										36.20	7.90	Door opening
	IF-RC-TG										18.50	3.90	Beam - infill gap
	IF-RC-SG	90	1350	980	RC	180×180	180×180	9.00	7650	16911	36.50	7.40	Columns - infill gaps
	IF-RC-ID										37.60	7.70	IP (1.37% d_r) + OoP
	IF-S				SS	W150 × 30	W150 × 30			201172	34.30	15.10	Steel frame
Domenico et al. (2018)	OOP_4E	80	2350	1830	RC	200×270	200×270	1.80	1517	32000*	4.09	5.40	All bounded
	OOP_3E										3.39	14.60	Beam - infill gap
	OOP_2E										8.42	17.00	Columns - infill gaps

* Estimated

Table 6: Analytical models developed for the estimation of infilled frame OoP capacity

#	Author	Ultimate load equation	Action	Remark																																				
1	Dawe and Seah (1989)	$w_1 = 0.8 \frac{f_m^{0.75} t^2 \alpha}{l^{2.5}} \quad (3)$	Gapped (w_1)	$\alpha = \frac{1}{h} (E_f I_c h^2 + G_f J_c t h)^{0.25}$																																				
		$w_2 = 0.8 f_m^{0.75} t^2 \left(\frac{\alpha}{l^{2.5}} + \frac{\beta}{h^{2.5}} \right) \quad (4)$	Two-way (w_2)	$\beta = \frac{1}{l} (E_f I_b l^2 + G_f J_b t l)^{0.25} \leq 50$																																				
2	Angel et al. (1994)	$w = R_1 R_2 \frac{2 f_m \lambda}{h/t} \quad (5)$	Two- & Gapped	<table border="1"> <thead> <tr> <th>h/t</th> <th>λ</th> <th colspan="2">R_1 by damage state (Fig.22)</th> </tr> <tr> <th></th> <th></th> <th>Moderate</th> <th>Severe</th> </tr> </thead> <tbody> <tr> <td>5</td> <td>0.129</td> <td>0.997</td> <td>0.994</td> </tr> <tr> <td>10</td> <td>0.060</td> <td>0.946</td> <td>0.894</td> </tr> <tr> <td>15</td> <td>0.034</td> <td>0.888</td> <td>0.789</td> </tr> <tr> <td>20</td> <td>0.021</td> <td>0.829</td> <td>0.688</td> </tr> <tr> <td>25</td> <td>0.013</td> <td>0.776</td> <td>0.602</td> </tr> <tr> <td>30</td> <td>0.008</td> <td>0.735</td> <td>0.540</td> </tr> <tr> <td>35</td> <td>0.005</td> <td>0.716</td> <td>0.512</td> </tr> </tbody> </table>	h/t	λ	R_1 by damage state (Fig.22)				Moderate	Severe	5	0.129	0.997	0.994	10	0.060	0.946	0.894	15	0.034	0.888	0.789	20	0.021	0.829	0.688	25	0.013	0.776	0.602	30	0.008	0.735	0.540	35	0.005	0.716	0.512
				h/t	λ	R_1 by damage state (Fig.22)																																		
		Moderate	Severe																																					
5	0.129	0.997	0.994																																					
10	0.060	0.946	0.894																																					
15	0.034	0.888	0.789																																					
20	0.021	0.829	0.688																																					
25	0.013	0.776	0.602																																					
30	0.008	0.735	0.540																																					
35	0.005	0.716	0.512																																					
				<p>Alternatively, R_1 can be calculated using Eq.13 In case of a gap: $R_2 = 0.357 + 2.488e-5 E_f I$ (use kN/m²) if $R_2 > 1 \Rightarrow R_2 = 1$ In case of no gap: $R_2 = 1.000$ (all sides connected)</p>																																				
3	Klingner et al. (1996)	$W = 8 \frac{M_{yv}}{h} (l - h) + 8 \frac{M_{yh}}{h} \ln(2) \left(\frac{x_{yv}}{x_{yh}} \right) \ln \left(\frac{l}{l - h/2} \right) l \quad (6)$	Two-way	<p>Use equation if $h/l \leq 2$ $x_{yv} = \frac{t f_m}{1000 E_m \left(1 - \frac{h}{2\sqrt{(h/2)^2 + t^2}} \right)}$ $M_{yv} = (0.85 f_m / 4)(t - x_{yv})^2$ For columns-infill (Double) gap use Eq. ??</p>																																				
4	Flanagan and Bennett (1999a)	$w = 0.73 f_m^{0.75} t^2 \left(\frac{a}{l^{2.5}} + \frac{\beta}{h^{2.5}} \right) \quad (7)$	Two-way	<p>$\alpha = \frac{1}{h} (E_f I_c h^2)^{0.25} \leq 50$ $\beta = \frac{1}{l} (E_f I_b l^2)^{0.25} \leq 50$ if $h/t < 8 \rightarrow t = h/8$</p>																																				
5	FEMA 356 (2000)	$w = 0.7 \frac{f_m \lambda_2}{h/t} \quad (8)$	Two-way	<table border="1"> <thead> <tr> <th>h/t</th> <th>5</th> <th>10</th> <th>15</th> <th>25</th> </tr> </thead> <tbody> <tr> <td>λ_2</td> <td>0.129</td> <td>0.060</td> <td>0.034</td> <td>0.013</td> </tr> </tbody> </table>	h/t	5	10	15	25	λ_2	0.129	0.060	0.034	0.013																										
h/t	5	10	15	25																																				
λ_2	0.129	0.060	0.034	0.013																																				
6	Moghaddam and Goudarzi (2010)	$w = \min \left\{ \begin{array}{l} w_{cr} = \frac{0.85 f_m}{(h/t)^2} - \left(0.12 + \frac{0.45}{\alpha} \right) \frac{f_m^2}{E_m} \\ w_{max} = \frac{0.18 E_m}{(0.12 + 0.045/\alpha)(h/t)^4} \end{array} \right\} \quad (9)$	<p>w_{cr} crushing failure Two-way w_{max} transverse instability failure</p>	$\alpha = \frac{384 E_f I_b h}{E_m t l^4}$																																				

Note: Use MPa and mm. The output of equations is in (MPa)

*For calculation of x_{yh} replace h with l , and for calculation of M_{yh} replace x_{yv} with x_{yh}

Table 7: Analytical solutions for ultimate OoP displacement

#	Author	Ultimate displacement	Remark
1	Klingner et al. (1996)	$x_y = \frac{tf_m l}{1000E \left(1 - \frac{h}{2\sqrt{(h/2)^2 + t^2}}\right)}$ (10)	
2	FEMA 273 (1997)	$d = \frac{0.002h^2/t}{1 + \sqrt{1 - 0.002(h/t)^2}}$ (11)	For $h/t \leq 22.3$
3	Flanagan and Bennett (1999b)	$d = \frac{0.002h^2/t}{1 + \sqrt{1 - 0.001(h/t)^2}}$ (12)	For $h/t \leq 31.6$

Dawe and Seah (1989) were the first to develop equations specifically for infilled frames. They developed two equations, for gapped (Eq. 3) and two-way (Eq. 4) action. The effects of frame's stiffness was introduced by the factors α and β . Parameter α considered the effects of columns; while β , beams. Within the one-way action equation (Eq. 3), parameter β was excluded due to the gapped arching-action. In other words, the beam is thus trivial in gapped arching-action. Furthermore, *Dawe and Seah (1989)* were the only equation developers that included the effects of frame's torsional characteristics.

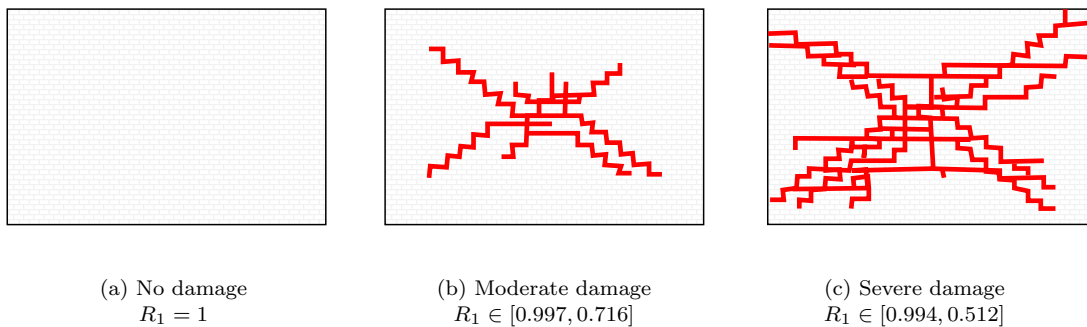
Angel et al. (1994) were the first and only developers of reduction factor (R_1 in Eq. 5) that resolves the degradation of OoP load-bearing capacity due to previous IP load. The reduction factors were based on damage states that can be determined; either visually, as illustrated in Figure 22, or by using Equation 13. The usage of previous IP damage factor is thus limited to the knowledge about the damage state or the displacement data, i.e. it is harder to estimate the damage state as it would be. Factor R_2 takes boundary conditions into the account. Whereas, if gapped arching-action occurs, the influence of the frame is introduced via $R_2 \leq 1$. Contrariwise, if the infill was fully bounded by the frame; $R_2 = 1$, the formula for capacity then resembles those of load-bearing URM walls without the frame. In other words, the effects of surrounding frame are thus omitted.

$$R_1 = 1 \text{ if } \frac{\delta}{2\delta_{cr}} < 0.5 \text{ i.e. undamaged state}$$

else

$$R_1 = \left[1.08 - 0.015 \frac{h}{t} - 0.00049 \left(\frac{h}{t}\right)^2 - 0.000013 \left(\frac{h}{t}\right)^3 \right] \frac{\delta}{2\delta_{cr}} \quad (13)$$

Where, δ is the maximum IP displacement, and δ_{cr} displacement at cracking load

Figure 22: Damage states for R_1 factor (Angel et al. (1994))

Klingner et al. (1996) develop an equation based on *Bashandy (1995)* model for load-bearing brickwork. *Klingner et al. (1996)* combined resistance from both vertical and horizontal arching-action, hence the indexes $_{yv}$ and $_{yh}$. Even though *Klingner et al. (1996)* did test infilled frames (Tab. 2), he did not include the effects of frames in his equation. From his load-bearing (Eq. 6), an ultimate OoP displacement equation can be derived (Eq. 10). Such equation is different from the other (Eq. 11& 12), as it included both geometrical and mechanical properties of the infill. Also, by removing horizontal or vertical arching-action from Equation 6, the resulting Equation 14 & 15 could be in essence, the first equation that can address the capacity of double gapped infilled frame.

$$W_{yv} = \frac{M_{yv}}{h}(l - h) \quad (14)$$

$$W_{yh} = 8 \frac{M_{yh}}{h} \ln(2) \left(\frac{x_{yv}}{x_{yh}} \right) \ln \left(\frac{l}{l - h/2} \right) l \quad (15)$$

Where the W_{yv} can be used for infill with both columns disconnected, and W_{yh} for infill with both beams disconnected.

Flanagan (1994) modified the two-way equation of *Dawe and Seah (1989)* (Eq. 4). The modification consisted of changing first constants, from 4.5 to 4.1; also, by removing torsional constants from α and β parameters. Additionally, *Flanagan (1994)* modified the equation of ultimate mid-height deflection from *FEMA 273 (1997)*, by changing the constant 0.002 to 0.001 under the square root.

FEMA 356 (2000); FEMA 273 (1997) uses a simplified version of *Angel et al. (1994)* equations, as published in: *Abrams et al. (1996)* paper. The simplification was ought by removing previous IP damage while considered infill bounded by all sides ($R_1 = R_2 = 1$). *FEMA 273 (1997)* also provided an equation for the calculation of mid-height deflections.

Moghaddam and Goudarzi (2010) as explained in section 2.1, proposed two modes of failures that were based on the infill's slenderness. Thick infills may crush at the boundaries w_{cr} while slender infills may collapse due to big transverse deflections w_{max} . Hence, w_{max} does not include masonry's compressive strength. The effects of frame are taken into the account by parameter α in form of stiffness.

There were no equations developed specifically for infilled frames that could include the effects of openings. However, *Mays et al. (1998)* developed an equation (Eq. 16) for load-bearing RC walls. Yet, the equation is used in a manner of firstly calculating the OoP capacity w with an arbitrary equation, and then reducing it with F_r factor and A_o/A_i ratio. Hence, it is reasonable to use it reduce the load-bearing capacity w of infilled frames. Furthermore, *Mays et al. (1998)* developed his equations for the calculation of blast, and not the seismic bearing capacities. Therefore, there is a mentioning of blast-resistant carpentry in Table 8.

$$w_o = w + wF_r \left(\frac{A_o}{A_i} \right) \quad (16)$$

Where F_r is selected from Table 8, w is an arbitrary equation used for calculation of OoP capacity (Tab. 6), A_i area of infill and A_o area of opening.

Table 8: Modification factor F_r for panels with openings (*Mays et al., 1998*)

Panel type	Blast-resistant openings	Opening location	F_r
One window	No	Central and offset	-1.00
One door	No	Central	+1.36
One door	No	Offset	-0.13
Two windows	No	Evenly distributed	-0.05
One window + one door	No	Evenly distributed	-0.41
One window	Yes	Central and offset	-3.07
One door	Yes	Central and offset	-2.73
Two windows	Yes	Evenly distributed	-2.62
One window + one door	Yes	Evenly distributed	-2.59

Notes on analytical models During the research of the analytical models, few discrepancies were observed. Therefore, readers may find equations here inconsistent with the would-be same equations in different articles. Mostly, the constants were changed because of difference in system of units (US or SI), or by units themselves (using MPa not kPa). For instance, in the original paper Dawe and Seah (1989) used the constant of 800; others referring to the same equation (Flanagan and Bennett, 1999a; Wang, 2017; Pasca et al., 2017) use the constant of 4.5. By recalculating the units, it was shown that constant of 800 is to be used when the f_m is in MPa and 4.5 when in kPa. In this paper; for the sake of uniformity, the constant was changed from 800 to 0.8 (Eq. 3 & 4). Hence, the output is in the same unit as are input parameters (MPa). Likewise, the original equation by FEMA 356 (2000), contains a constant of 144; however, when f_m is converted from psi to MPa, the constant changes to $0.99 \approx 1.00$ as is used in paper by Pasca et al. (2017). Authors here modified all equations in order to have all the input in MPa and mm resulting in MPa output

3.1 Analytical models analysis input

The analytical model analysis was carried out on the mechanical and geometrical characteristics of the specimens listed in the Table 5. Parametric analysis was carried out on Sepasdar (2017) IF-ND specimen, as it showed the greatest correlation with all analytical models.

When calculating torsional constants of rectangular sections, equation 17 along with Table 10 were used. Contrariwise, in case of non-rectangular (steel) sections, the constant was extracted from catalogues found on Tools for Engineer website (2019).

Furthermore, for the purpose of parametric, i.e. sensitivity analysis a range of values was established and presented in Table 9. Though, when parameters such as $h/t \in [5, 35]$ could not be incorporated as a single variable, thickness was set to the original value of $t = 90$ mm while the value of height was obtained as a range with $h = t \cdot h/t$. Analogously for aspect ratio h/l , where h was set as a constant so the slenderness is not influenced. In case of modifying masonry's compressive strength, elastic modulus (E_m) was altered with the use of Equation 18.

Table 9: Range of parameter values that are considered for the parametric analysis

Parameter	Range
Slenderness	$h/t \in [5, 35]$
Aspect ratio	$l/h \in [0.5, 3.0]$
Frame element section size	$b_b \in [50, 500]$ mm
Masonry's compressive strength f_m	$f_m \in [1, 35]$ MPa

$$J = \beta ab^3 \quad (17)$$

Where β is obtained trough linear interpolation by using Table 10

Table 10: Values of β for torsional constant J (Ugural and Fenster, 2003)

a/b	1.000	1.500	2.000	2.500	3.000	4.000	5.000	6.000	10.000	∞
β	0.141	0.196	0.229	0.249	0.263	0.281	0.291	0.299	0.312	0.333

$$E_m = f_{m,k} \cdot K_E \quad (18)$$

Where K_E is 1000 in accordance with Annex of EN1996-1-1 provision (BSI, 2004).

3.2 Analytical model analysis results

The results of calculated data is presented in Tables 11, 13, 14, 15 and Figures 23, 24 and 26.

Table 11 shows the overall absolute difference grouped by various properties and equations. Table 13 shows calculated capacities of various specimens as listed in Table 5, while Table 14 shows, a difference between experientially and analytically obtained load-bearing capacities. Likewise, Table 13 shows calculated values, while Table 15 the differences of displacements.

Figure 24 displays the difference of each specimen by equations, the upper limit was set to 900 %. Hence, some models outside the range were omitted from the plot. Likewise, Figure 26 presents the differences of various properties in regards to an arbitrary analytical model. Error variabilities are presents in Figure 23. It shows the extremes, quartiles and medians. Note that the box diagram of Moghaddam and Goudarzi (2010) had a misaligned median, that is outside the quartiles. It is by the reason of choosing the minimal value between w_{cr} and w_{max} .

The results of single-variable parametric analysis are shown in Figure 27 with left side showing the results of two- and right one-way actions. Note that Figure 27c has lower limit set to -0.2 and upper set 0.4 MPa.

Multi-variable parametric analysis is displayed on Figure 28. On left sides, axonometric, while on the right side, topographic projections were plotted.

All differences were calculated by the use of Equation 19.

$$\Delta w = \frac{w_{\text{analytical}} - w_{\text{experiment}}}{w_{\text{experiment}}} \quad (19)$$

Klingner et al. (1996) curve in Figure 27a shows results in domain of $h/t < 30$ as for aspect ratio of $h/l < 2$, natural logarithm $\ln(l/(l-h/2))$ (Eq. 6) produced complex numbers \mathbb{C} due to $\ln(\mathbb{R}^-)$. Likewise, as a result of negative values under the square root, Equations 12 & 11 produce complex numbers (Fig. 29). Therefore, they are restricted to the values of $h/t > 31.6$ and > 22.3 , respectably. All the limitations were incorporated in Tables 6 and 7 in order for readers of this paper to have insight in advanced.

Table 11: Absolute difference in equations outputs by various properties

Property	Difference by equation (%)					
	Eq. 5	Eq. 3 & 4	Eq. 7	Eq. 9	Eq. 8	Eq. 6
Total	205.71	71.44	61.04	39.41	96.12	228.87
RC frame	100.55	52.42	53.65	50.84	67.69	49.25
SS frame	400.99	89.00	66.16	31.49	115.81	380.86
Plain masonry panel	261.07	81.02	64.97	40.58	103.95	231.66
Beam - infill gap	155.00	55.74				
Columns - infill gaps						43.78
Openings	197.25	51.25	47.97	37.50	56.44	145.71
Concrete units	377.81	80.01	69.40	35.47	112.68	352.20
Clay units	78.50	60.53	48.96	45.10	72.20	56.22

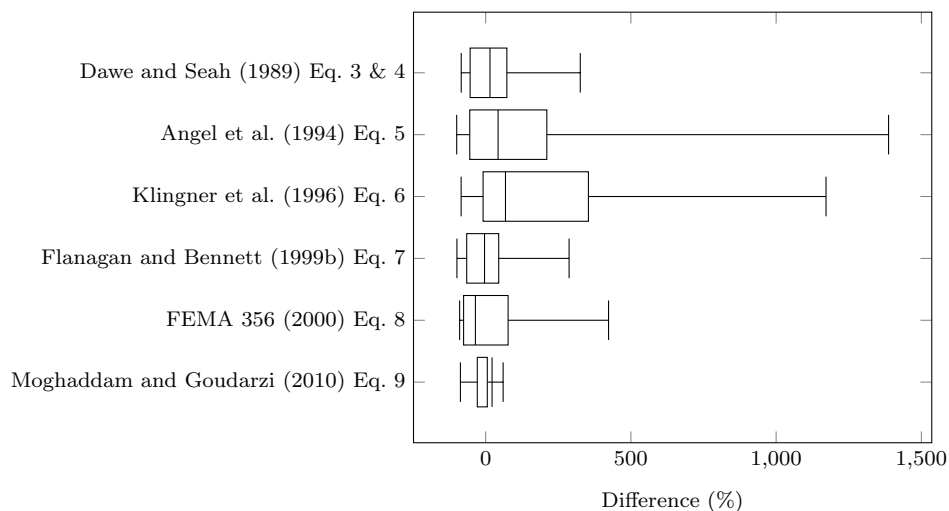


Figure 23: Variation of differences plotted as quartiles between various analytical models

Table 12: Calculated OoP capacities

Author	Specimen	Calculated OoP capacity by equation (kPa)							Remark	
		Eq. 3 & 4	Eq. 5	Eq. 6	Eq. 7	Eq. 8	Eq. 9			
		w_{cr} w_{max}								
Dawe and Seah (1989)	WE1	33.20	116.00	99.20	30.20	40.80	-736.20	27.20	Trust type joint reinf.	
	WE2	33.20	116.00	99.20	30.20	40.80	-736.20	27.20	Plain masonry panel	
	WE3	33.20	116.00	99.20	30.20	40.80	-736.20	27.20	Dry-stack panel	
	WE4	18.00	51.00	53.80	16.40	17.90	-561.90	10.90	Plain masonry panel	
	WE5	7.40	11.50	22.20	6.80	4.00	-374.50	2.90	Plain masonry panel	
	WE6	30.30	116.60	99.20	0.15	40.80	-736.20	27.20	Plain masonry panel	
	WE7	30.30	116.60	99.20	0.15	40.80	-736.20	27.20	Truss type joint reinf.	
	WE8	18.00	51.00	53.80	16.40	17.90	-561.90	10.90	Restraints against slipp.	
	WE9	26.89	93.96	80.35	24.46	33.05	-596.32	22.03	Window opening	
Angel et al. (1994)	1	4.80	3.80	9.00	4.40	1.30	-30.90	4.80	Pure OoP. S mortar	
	2		1.80						IP (0.34% dr) + OoP, N mort.	
	3		1.70						IP (0.22% dr) + OoP, L mort.	
	4		5.50						IP (0.09% dr) + OoP, N mort.	
	5		5.10						IP (0.06% dr) + OoP, N mort.	
	6		0.79						IP (0.25% dr) + OoP, L mort.	
	7		1.90						IP (0.25% dr) + OoP, N mort.	
	8		0.60						IP (0.39% dr) + OoP, L mort.	
Flanagan and Bennett (1999a)	25	9.30	6.70	11.40	8.50	2.40	5.90	8.50	Plain masonry panel	
18	40.90	51.00	50.00	37.30	17.80	32.00	957.60	32.00	Plain masonry panel	
22	68.30	70.40	58.60	44.80	24.60	30.10	13318.90	30.10	Plain masonry panel	
19		50.30							IP (0.8% dr) + OoP	
Hak et al. (2014)	TA1		31.80						IP (1.50% dr) + OoP	
TA2			29.00						IP (2.00% dr) + OoP	
TA3			29.00						IP (1.00% dr) + OoP	
Akhoundi et al. (2016)	SIF-A	1.40	4.70				0.00		Beam - infill gap	
SIF-B	3.50	4.70	4.00	3.20	1.60	2.20	24.00		Plain masonry panel	
PIF-A	2.80	3.76	3.20	2.56	1.28	1.76	19.20		Window opening	
Furtado et al. (2016)	inf.01	2.40	2.30	2.10	2.20	0.80	1.80	104.00	OoP mono. + gravity load	
inf.02	2.40	2.30	2.10	2.20	0.80	1.80	104.00	104.00	OoP cyclic	
inf.03		2.00							OoP cyclic + IP (0.5% dr)	
Sepasdar (2017)	IF-W	42.91	75.95	55.11	36.27	26.56	36.27	439.82	439.82	Window opening
IF-ND	51.70	91.50	66.40	46.80	32.00	43.70	529.90	529.90	Plain masonry panel	
IF-D1		86.00							IP (0.66% dr) + OoP	
IF-D2		79.80							IP (2.70% dr) + OoP	
Wang (2017)	IF-RC-DO	64.07	113.40	82.29	58.00	39.66	54.16	656.74	656.74	Door opening
	IF-RC-TG	17.80	91.50							Beam - infill gap
	IF-RC-SG			35.40						Columns - infill gaps
	IF-RC-ID		79.80							IP (1.37% dr) + OoP
	IF-S	63.50	91.50	66.40	57.90	32.00	54.90	1239.20	1239.20	Steel frame
Domenico et al. (2018)	OOP_4E	1.90	2.60	3.00	1.70	0.90	-2.20	4.40	4.40	All bounded
OOP_3E	0.71	2.60							Beam - infill gap	
OOP_2E			1.30						Columns - infill gaps	

Table 13: Calculated OoP displacement

Author	Specimen	Calculated values (mm)			Remark
		Eq. 10	Eq. 11	Eq. 12	
Flanagan and Bennett (1999a)	25	64.18	∈ C	65.48	Plain masonry panel
	18	31.14	27.70	26.64	Plain masonry panel
	22	8.24	15.57	15.38	Plain masonry panel
Akhoundi et al. (2015)	SIF-B	29.74	27.82	25.82	Plain masonry panel
Furtado et al. (2016)	inf.01	42.20	40.82	37.63	OoP monotonic + gravity load 300 kN
	inf.02	42.20	40.82	37.63	OoP cyclic
Sepasdar (2017)	IF-ND	8.69	11.39	11.01	Plain masonry panel
Wang (2017)	IF-S	8.69	11.39	11.01	Steel frame
Domenico et al. (2018)	OOP_4E	58.70	∈ C	49.53	All bounded

Table 14: Differences between calculated and experimental OoP capacities

Author	Specimen	Difference (%)							Remark
		Eq. 3 & 4	Eq. 5	Eq. 6	Eq. 7	Eq. 8	Eq. 9 w_{cr}	w_{max}	
Dawe and Seah (1989)	WE1	48.88	420.18	344.84	35.43	82.96	-3401.35	21.97	Trust joint reinf.
	WE2	72.92	504.17	416.67	57.29	112.50	-3401.35	21.97	Plain masonry panel
	WE3	325.64	1387.18	1171.79	287.18	423.08	-3401.35	21.97	Dry-stack panel
	WE4	60.71	355.36	380.36	46.43	59.82	-2619.73	-51.12	Plain masonry panel
	WE5	-5.13	47.44	184.62	-12.82	-48.72	-1779.37	-87.00	Plain masonry panel
	WE6	185.85	1000.00	835.85	-98.61	284.91	-3401.35	21.97	Plain masonry panel
	WE7	106.12	693.20	574.83	-99.00	177.55	-3401.35	21.97	Trust joint reinf.
	WE8	34.33	280.60	301.49	22.39	33.58	-2619.73	-51.12	Restraints against slipp.
	WE9	54.55	440.00	361.79	40.59	89.93	-2774.09	-1.20	Window opening
Angel et al. (1994)	1	-41.39	-53.60	9.89	-46.28	-84.13	-477.29	-41.39	Pure OoP, S mort.
	2		-55.22						IP (0.34% dr) + OoP, N mort.
	3		-71.62						IP (0.22% dr) + OoP, L mort.
	4		-81.53						IP (0.09% dr) + OoP, N mort.
	5		-84.17						IP (0.06% dr) + OoP, N mort.
	6		-93.67						IP (0.25% dr) + OoP, L mort.
	7		-93.82						IP (0.25% dr) + OoP, N mort.
	8		-98.13						IP (0.39% dr) + OoP, L mort.
Flanagan and Bennett (1999a)	25	14.81	-17.28	40.74	4.94	-70.37	-27.16	4.94	Plain masonry panel
	18	53.76	91.73	87.97	40.23	-33.08	20.30	3500.00	Plain masonry panel
	22	72.91	78.23	48.35	13.42	-37.72	-23.80	33618.73	Plain masonry panel
	19		131.80						IP (0.8% dr) + OoP
Hak et al. (2014)	TA1		-99.76						IP (1.50% dr) + OoP
	TA2		257.45						IP (2.00% dr) + OoP
	TA3		122.85						IP (1.00% dr) + OoP
Akhoundi et al. (2016)	SIF-A	-84.21	-46.98						Beam - infill gap
	SIF-B	-65.45	-53.60	-60.51	-68.41	-84.21	-78.28	136.91	Plain masonry panel
	PIF-A	-71.65	-61.93	-67.60	-74.08	-87.04	-82.18	94.39	Window opening
Furtado et al. (2016)	inf_01	-69.09	-70.38	-72.95	-71.66	-89.67	-76.82	1239.52	OoP mono. + gravity load
	inf_02	-66.88	-68.26	-71.02	-69.64	-88.93	-75.16	1335.20	OoP cyclic
	inf_03		13.65						OoP cyclic + IP (0.5% dr)
Sepasdar (2017)	IF-W	-1.81	73.79	26.11	-17.00	-39.22	-17.00	906.45	Window opening
	IF-ND	-22.02	38.01	0.15	-29.41	-51.73	-34.09	699.25	Plain masonry panel
	IF-D1		93.69						IP (0.66% dr) + OoP
	IF-D2		202.27						IP (2.70% dr) + OoP
Wang (2017)	IF-RC-DO	77.00	213.26	127.33	60.23	9.56	49.61	1714.19	Door opening
	IF-RC-TG	-3.78	394.59						Beam - infill gap
	IF-RC-SG			-3.01					Columns - infill gaps
	IF-RC-ID		112.23						IP (1.37% dr) + OoP
	IF-S	85.13	166.76	93.59	68.80	-6.71	60.06	3512.83	Steel frame
Domenico et al. (2018)	OOP_4E	-53.57	-36.47	-26.70	-58.46	-77.93	-153.76	7.51	All bounded
	OOP_3E	-79.23	-23.42						Beam - infill gap
	OOP_2E			-84.56					Columns - infill gaps

Table 15: Difference between analytical models and experimental OoP displacement

Author	Specimen	Eq. 10 %	Eq. 11 %	Eq. 12 %	Remark
Flanagan and Bennett (1999a)	25	153.67	∈ C	158.81	Plain masonry panel
	18	170.79	140.86	131.66	Plain masonry panel
	22	-57.32	-19.31	-20.29	Plain masonry panel
Akhoundi et al. (2016)	SIF-B	147.86	131.83	115.14	Plain masonry panel
Furtado et al. (2016)	inf_01	91.84	85.55	71.03	OoP monotonic + gravity load 300 kN
	inf_02	251.70	240.18	213.55	OoP cyclic
Wang (2017)	IF-S	-42.46	-24.56	-27.10	Steel frame
Sepasdar (2017)	IF-ND	-42.46	-8.86	-27.10	Plain masonry panel
Domenico et al. (2018)	OOP_4E	986.99	∈ C	817.16	All bounded

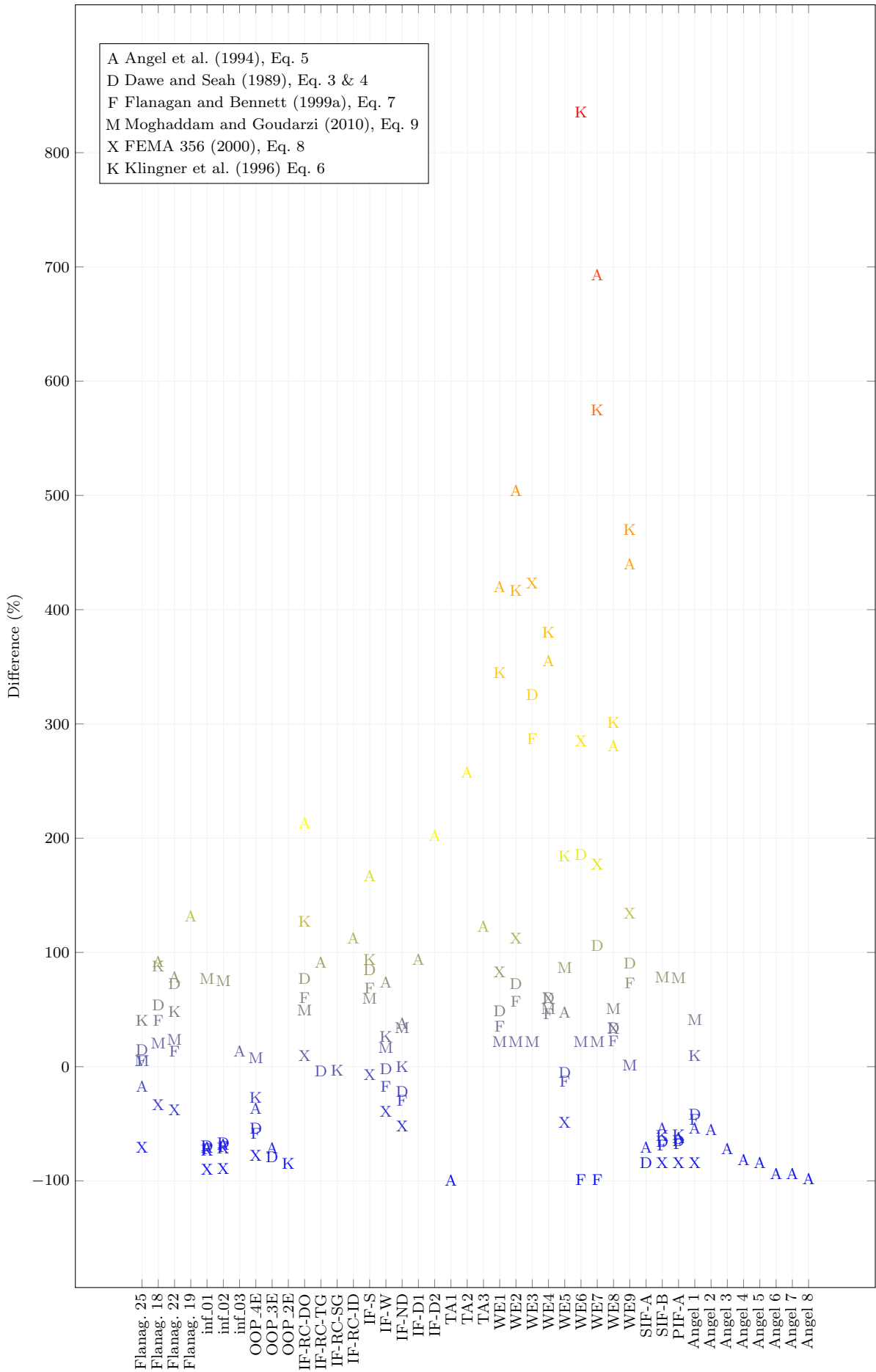


Figure 24: Differences of various analytical models for each specimen

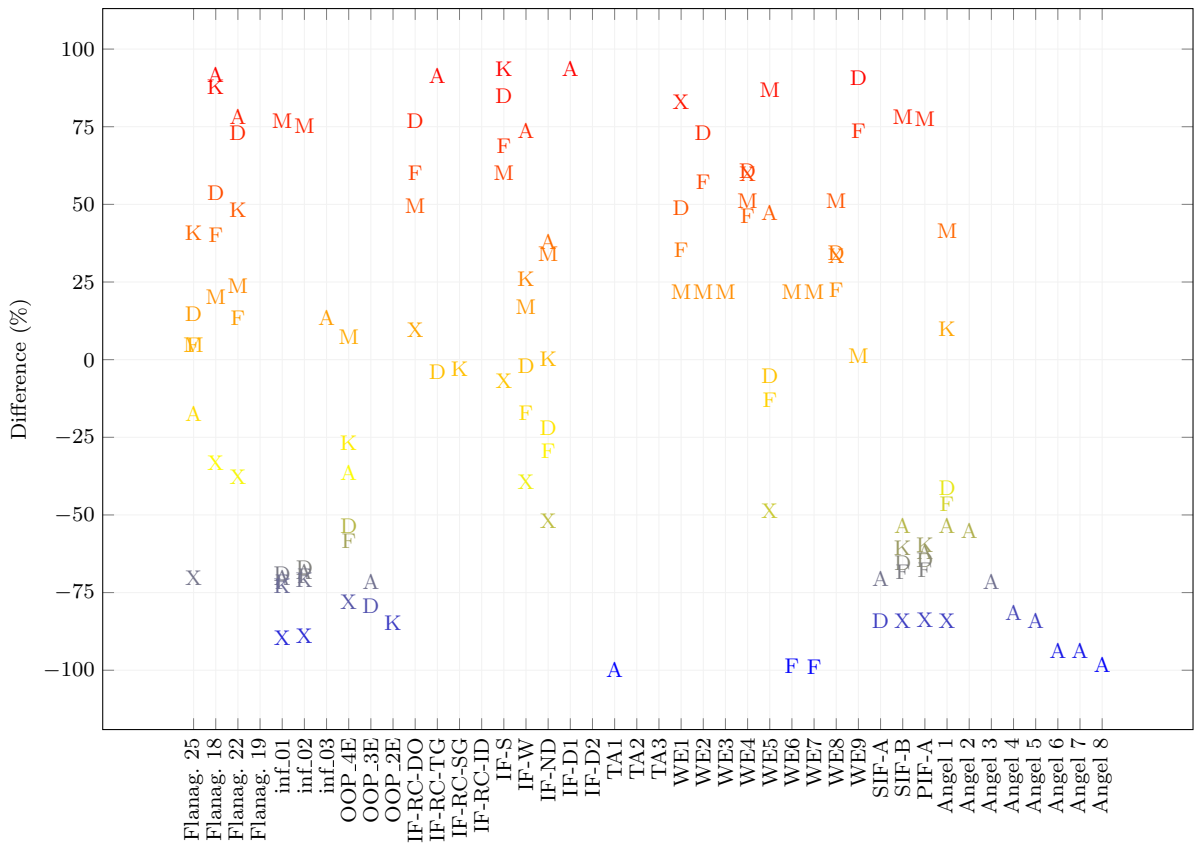


Figure 25: Enlarged section of Fig. 24

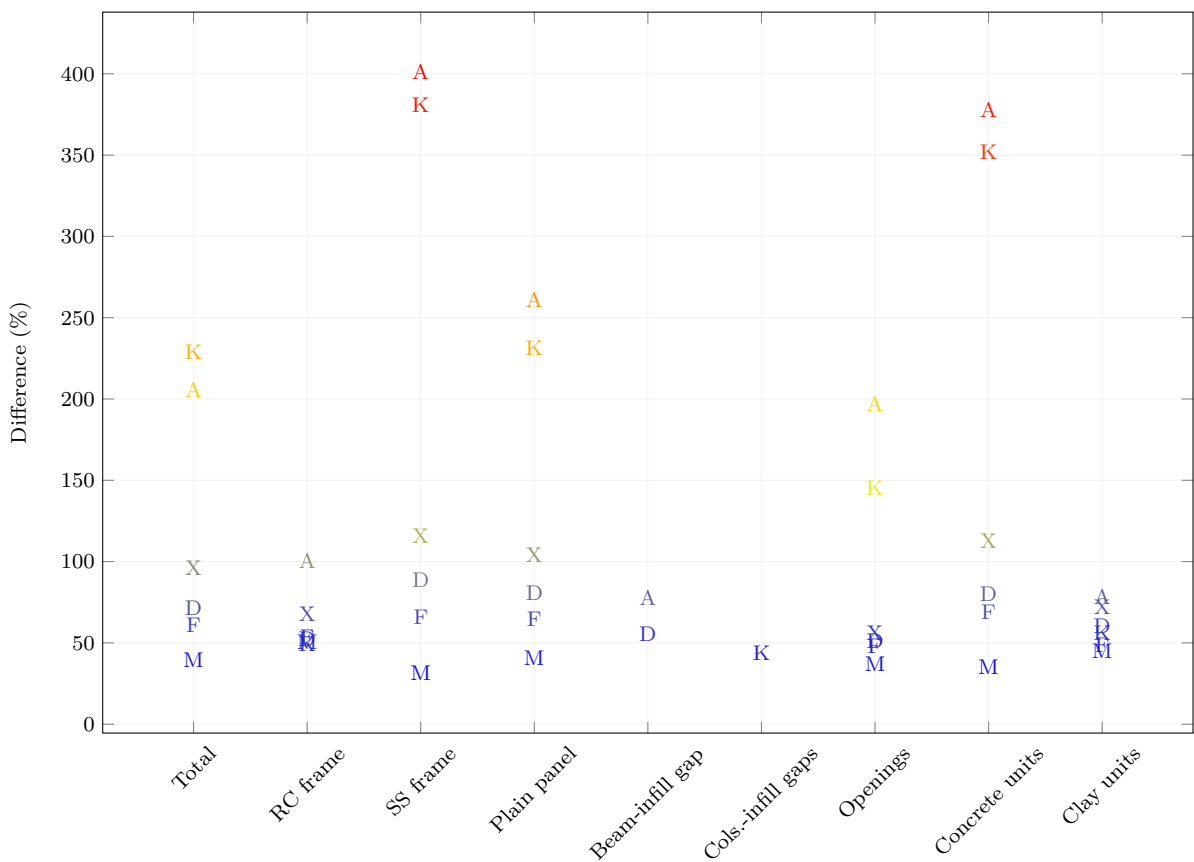
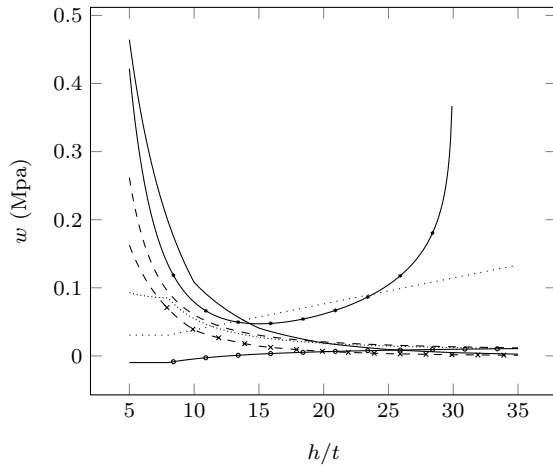


Figure 26: Absolute differences of various analytical models by specific property (legend as in Fig. 24)



(a) Effects of slenderness on two-way action

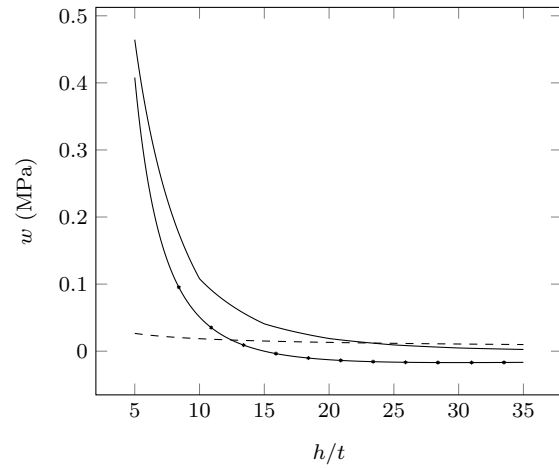
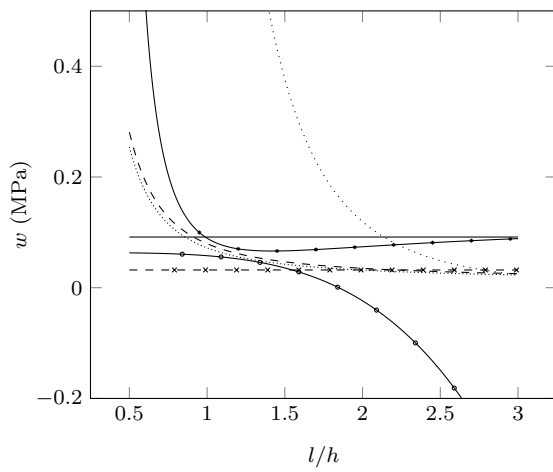
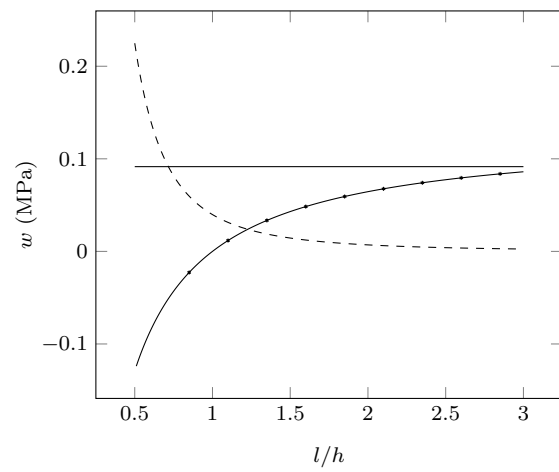
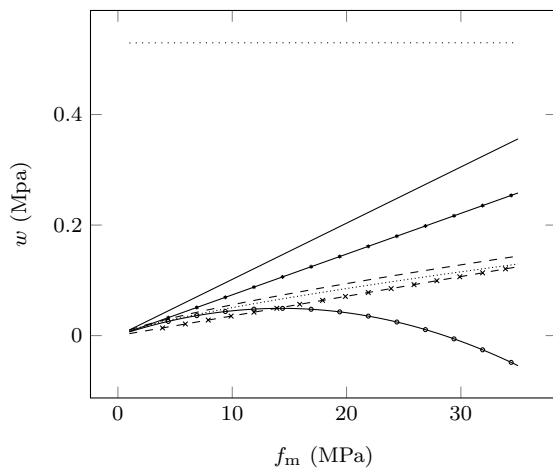
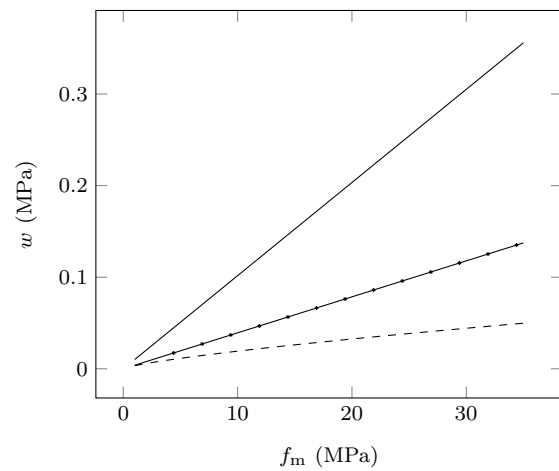
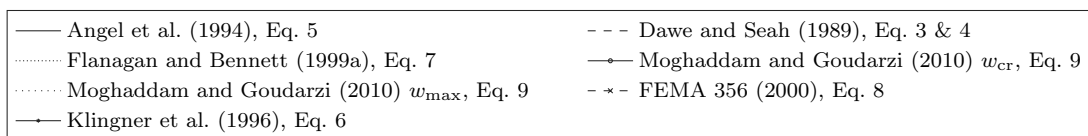
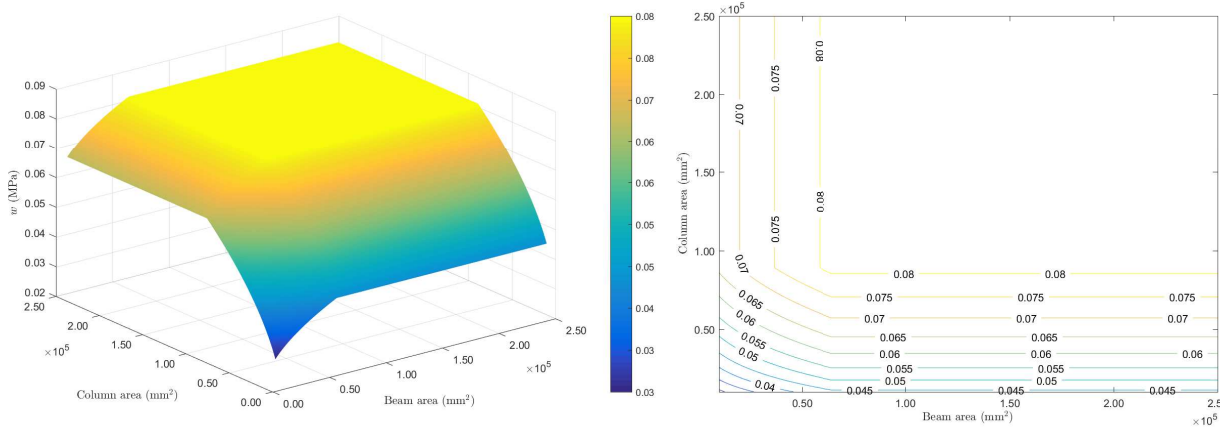
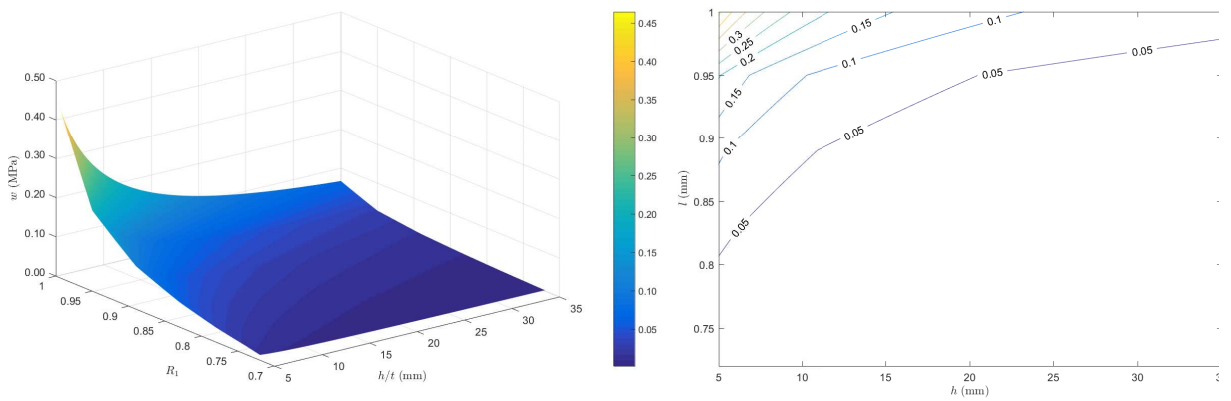
(b) Effects of slenderness (h/t) on one-way action(c) Effects of aspect ratio (l/h) on two-way action(d) Effects of aspect ratio (l/h) on one-way action(e) Effect of compressive strength (f_m) on two-way action(f) Effect of compressive strength (f_m) on one-way action

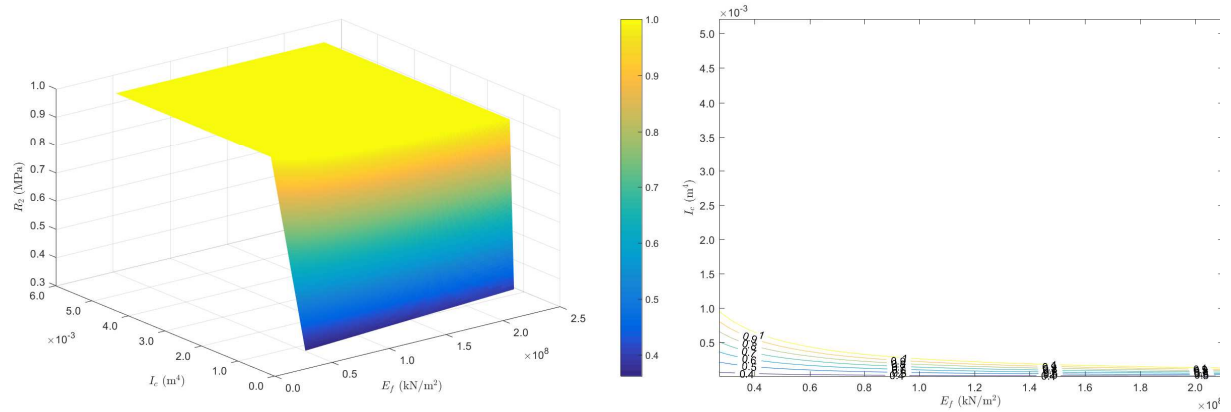
Figure 27: Single-variable parameter sensitivity analysis of analytical models



(a) Effects of section size on Dawe and Seah (1989) equation 3



(b) Effects of prior IP damage (R_1) and slenderness (h/t) on Angel et al. (1994) equation 5



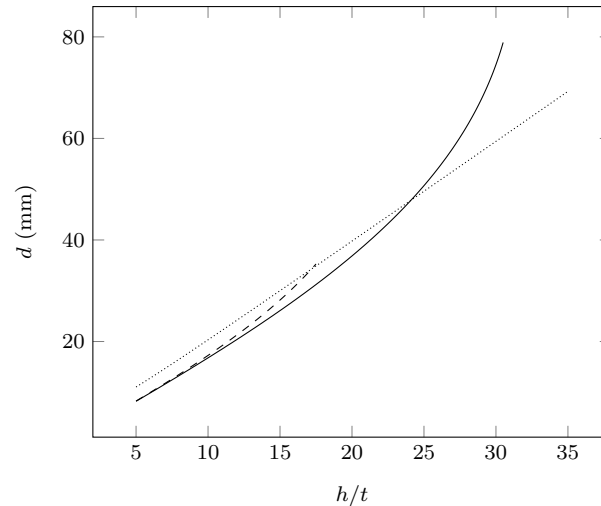
(c) Effects of moment of inertia (I) and elastic modulus of frame (E_f) on R_2 coefficient from Angel et al. (1994) equation 5

Figure 28: Multi-variable parameter sensitivity analysis of analytical models

4 Discussion & overview

4.1 Experimental studies

There are three main experimental methods: 1) inertial ; 2) inter-storey drift and 3) dynamic. Dynamical methods are certainly the best option for understanding the behaviour of framed masonry structures under seismic load. However, they are more expensive and require more sophisticated equipment (as



— Flanagan and Bennett (1999b) Eq. 12 - - - FEMA 273 (1997) Eq. 11 Klingner et al. (1996) Eq. 10

Figure 29: Effects of slenderness (h/t) on ultimate OoP displacement calculations

shaking table). Thus, simpler methods are used; namely, inertial and inter-storey drift methods. Both remark the specific forces that would act upon a structure given an earthquake scenario.

From Tables 2 - 4 and Figures 5 - 7 it can be observed that most experiment were done with inertial-cyclic method; and approximately, half had previous cyclic IP load. Most frames were made from RC, while infills were made using clay masonry, laid in a manner so the voids were facing vertical direction. Infill's slenderness was in the range of $h/t \in [1.35, 39.68]$ with the majority of them below the BSI (2005) limit for special actions (11.20 median). The aspect ratio was in the range of $l/h \in [0.58, 2.00]$, with the median of 1.36. One tested opening in the area of negligence, while the rest were in above. From Figure 21, it can be observed that masonry's compressive strength was in the range of $f_m \in [0.53, 24.30]$ MPa with the median of 9 MPa. Very low f_m 'm were mainly from Portuguese researches where traditionally, block have low strength that can be attributed to the fact that they are laid horizontally. Likewise, the masonry's elastic modulus was in the range of $E_m \in [942, 17575]$ MPa with the median of 5300 MPa. The previous IP inter-storey drift was applied in the range of $d_r \in [0.06, 2.70]$ % with the median of 0.39 %.

Investigating different kinds of loadings, it was found that there are considerable differences between the inertial and inter-storey drift methods. Namely, the inertial methods damaged the infill, while leaving the frame intact; contrariwise, the inter-storey drift methods, damage the frame while slightly damaging the infill. Furthermore, there are more matchings between the inter-storey drift and dynamical methods. For instance, it was found that frame and infill move as a single unit and the damage states both have frames significantly more damaged in contrast to the infill. Also, it was shown that infill had greater acceleration and/or the same displacements when compared to the frame. Hence, infill walls were more susceptible to inertial forces. Along with the infill walls proneness to inertial effects and the fact that with dynamical excitation, frame and infill act as one; it is expected that inertial failure occurs when there is a loss in boundary conditions. For example, it is common that due to in-plane loads a connection between the beam and the infill wall is lost. Hence, when imposing out-of-plane loads the frame and infill would not work as a single unit. As a consequence, infill wall would fall out, resulting in an inertial failure. Likewise, the same can occur as a consequence of poor workmanship. As it is challenging for workers to fill the void between beam and the infill wall. Withal, the role of the frame even with the fallen infill should be addressed. In like manner, few researches removed the connection between columns and infill. Such boundary conditions are by some referred as *practical considerations*; since infill and frame would behave more or less independently from each other.

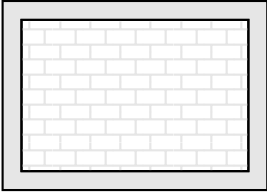
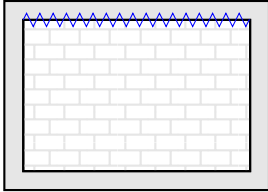
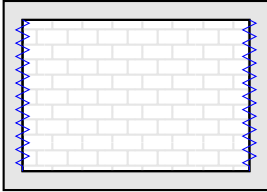
With pure out-of-plane inertial methods, an analogy with plate structures was determined. In other words, it had similar yield patterns when it comes to boundary condition and resists the transverse through membrane forces as the infill wall do trough arching-action.

The main discovery of the field was certainly the development of *arching-action*. Arching-action is what renders membrane forces in regards to plate analogy. Namely, when the infill is loaded, it bends. After reaching the critical point, the infill cracks. Thus, the infill splits in two separate parts that clamp on contacting surfaces while open on the opposing. Those three clamping points (mid-height and supports)

form the *three-hinged arch*. Named after the same resisting mechanism of an arch with three hinges. The arching-action resists transverse forces with additional compressive, normal forces. Through arching-action, infill can withstand capacities up to six times than those predicted by flexural theory. Aside of three-hinged arching action, a two- and four-hinged arching-actions were discovered. The two-hinged arching-action was found in the dynamical test, and is a probable action of inter-storey drift methods. Certain factors can bypass or limit the arching-action, such as: boundary conditions; slenderness, aspect ratio; gravity loads; infill type; mortar type; previous actions; openings and etc.

Boundary conditions, sometimes refereed as *effects of workmanship* or *practical considerations* have shown significant impact on out-of-plane behaviour. In other words, with every loss of interface, there is loss in bearing and deformation capabilities. Also, it affects the yielding patters, and failure modes. On one hand, with all sides connected to the frame *two-way* or *rigid* (vertical and horizontal) arching-action is achieved. On the other hand, with one (beam-infill) or two (columns-infill) interfaces missing, an *one-way* or *gapped* (vertical) arching-action is developed. Authors here would recommend not using the term one-way arching for single gapped systems, as it can lead the conclusion that it does not contain both vertical and horizontal arching. Hence, the recommended terminology is shown in Table 16.

Table 16: Recommended terminology

		
Fully connected Two-way arching Rigid arching action	Partly connected / Single gapped or gapped arching action	One-way arching Double gapped arching action

Seven studies were carried out that have observed the effects of openings. Those studies included: 1 door, 4 window and 2 full height openings, placed centrally. All showed a drastic reduction of deformational capabilities. However, in regards to bearing capacities, 3 out of 5 studies shown a decrease and 2 showed no change in bearing capacity. The reduction was observed on door, window and a full height openings. While two window openings shown no decrease in ultimate force. The reason for such discrepancy is yet to be found. However, the reason could lay in the lintel, as numerical studies have shown that the existence of lintel add an additional point to the compression arch. Furthermore; yield patterns have revealed that even with openings, the arching-action was able to develop. However, its effectiveness was limited.

Both infill's slenderness and the aspect have shown effects on the out-of-plane behaviour. As the arching-action is a function of compressive forces, it is intuitive that slenderness and aspect ratios could lower or elevate the infill's bearing and deformation capacities. Also, it was found that; depending on slenderness, the infill may fail due to transverse instability or by crushing at boundary. In other words, with thick infills the arching-action could be bypassed.

4.2 Analytical models

There were 6 analytical models developed for the calculation of infilled frames, load-bearing capacities (Tab. 6). All of them were developed on the basis of inertial experiments. However, equation 10 by Flanagan and Bennett (1999a) was a modification pre-existing equations 4 by Dawe and Seah (1989), while FEMA 356 (2000) uses simplified equation from Shapiro et al. (1994). Hence, 4 analytical models were originally developed. Each model had a specific effect accounted for, such as: previous in-plane damage, one- or/and two-way action, torsion of frame parts, different modes of failure. Out of those 6 equations, 5 of them include the effects of surrounding frame, mainly through stiffness. Note that, there were also flexural-action based analytical models. However, they were discarded and not covered within this paper.

It was found that, deflection and load-bearing equations differ greatly, among themselves and with the experimental data. The greatest, overall performance of load bearing equation was that of Moghaddam

and Goudarzi (2010) (Eq. 9). There, two modes of failure were addressed; namely, the transverse instability and crushing at the boundaries. Minimal value between the two was the governing one. In most cases, the transverse instability failure was the prevailing one. Hence, the arching-action was present in most cases. Furthermore, authors of this paper had extracted a pure one-way action from Klingner et al. (1996) equation 6. The equation was used to calculate load-bearing capacities of specimens with columns - infill gap. The capacities had 43 % difference from the experimental ones. However, when compared to the other capacities, the equation was near enough to present a possibility of its further development.

The parametric, i.e. sensitivity analysis had revealed few stability issues. Namely, the load-bearing equation 6 and displacement equations 12 & 11 had in few instances, negative numbers under the square root resulting in complex number outputs. Hence, authors of this paper have incorporated the newly found limits within the equations remarks (Tab. 6 & 7).

Furthermore, parametric analysis yielded that slenderness, aspect ratio and compressive strength have great influence on the equation outputs. However, slenderness and compressive strength did not have a greater role in all equations when compared with aspect ratio. Compressive strength had a more; uniformly linear response, contrarily to the effects of slenderness and aspect ratio. Slenderness had greater differences with thick infill walls; whereas, lower for slender ones. This fact goes in hand with the Moghaddam and Goudarzi (2010) principal. Slender infill walls fail as a result of excessive transversal deflection, i.e. arching action. While, thick infill walls fail not from the arching-action; rather, by crushing at the supports. Hence, as all equations were arching-action based, the best correlations were in the domain where slenderness was greater. Furthermore, the effects of frame were addressed through column's and beam's cross-sectional size. The effects were minimal; hence, the omitting of torsional effects from Equation 4 were justified in the modification of Equation 4 by Flanagan and Bennett (1999b) in Equation 7. Similarly, the effects of frame in the case of one-way action of equation 5 by Angel et al. (1994) are minimal; and in case of two-way action non-existing. Overall, the frame had substantially low impact on the equations output, as is the case of inertial experimental methods. Hence, the absence of frame's influence in Equation 6 by Klingner et al. (1996) is upheld. Furthermore, previous in-plane damage along with slenderness affect the outcome of Equation 5 greatly. The same is revisable in the experimental reports.

5 Conclusions

High-rise buildings are frequently composed of load-bearing frames, and non-bearing infill walls. During an earthquake, inertial and inter-storey drift forces act upon such structures, forcing the interaction between the two. Thus, rendering the behaviour of the frame and with it, whole structure. In real earthquake scenario, those forces act both in in- and out-of-plane direction. Thus, for better understanding of such behaviour, the field of research was divided in three principal sub-fields: in-plane, out-of-plane and the bidirectional behaviour. The bidirectional behaviour regards the effects of: previous in-plane damage on out-of-plane behaviour; previous out-of-plane damage on in-plane behaviour and simultaneous in-plane and out-of-plane action.

This paper has revised the literature in regards to the pure out-of-plane and bidirectional seismic loading. Also, this paper scoped experimental and analytical models. Paper's focal point was set on the field of seismic engineering and infilled frames, while also focusing on effects of openings. However, due to similarities, there are few occasions of referencing blast engineering and load-bearing walls (without the frame) studies.

There are three basic out-of-plane methods for testing infilled frames: dynamic, inertial and inter-storey drift methods. The inertial method was the most common practice, mostly done with air-bags. The inter-storey drift method is poorly researched, as are dynamical methods.

It was found that during the out-of-plane, inertial loading, a beneficial arching-action occurs. With it, additional compressive forces are in effect and thus, providing supplementary resistance to the transversal ones. The only mentioning of arching-action in dynamical methods was the subordinate, two-hinged action. In the case of inter-storey drift methods, there were no mentioning of arching-action.

It was found that inertial and inter-storey drift methods differ greatly. Namely, the inertial methods damage the infill and frame, only slightly. The exact opposite is true with inter-storey drift method. In dynamical methods, it was found that the frame and infill move as a single unit, and the frame was more damaged. Furthermore, infill had higher accelerations than the frame. Hence, soon as infill loses connection to the frame (i.e. due to previous in-plane drift) they do not act as a single unit. Thus, an inertial failure of infill may occur;

Various parameters can limit or bypass arching action as: slenderness, aspect ratio, boundary conditions, gravity load, masonry and mortar type, openings, frame stiffness.

Analytical models produce widely dispersed results. Slenderness and compressive strength of the infill have shown the greatest influence on ultimate force. The equation for the calculation regarding the effects of openings by Mays et al. (1998), was shown to be inadequate. The best correlations with analytical and experimental outputs were found with equation 9 by Moghaddam and Goudarzi (2010).

More research should be focused on inter-storey drift method and/or the combination of inter-storey drift and inertial methods. Also, as were no studies done on the effects of inter-storey drift method on reinforced concrete frames. Ergo, such experimental campaign should be addressed.

More studies should include the effects of simultaneous out-of-plane and in-plane loading. Also, the effects of previous out-of-plane damage on in-plane behaviour should be updated.

There is a need for a systematic study on the effects of openings. Especially for the dynamical and inter-storey drift methods as there are none. The effects of confined openings should be addressed within all methods.

It is unclear as in what type (if any) of arching-action is formed with dynamical and inter-storey drift methods. Hence, a focus of such should be addressed.

More research should be done with out-of-plane behaviour of multi-storey and/or multi-bay structures.

Also, there is a demand for the development of an *universal equation* for inertial methods that will cover most of parameters that govern the OoP behaviour. Also, there should be further effort for the development of analytical models based on dynamical and inter-storey drift methods and/or their combinations.

Acknowledgements The research presented in this article is a part of the research project FRAMed-Masonry composites for modelling and standardization (HRZZ-IP-2013-11-3013) supported by Croatian Science Foundation and its support is gratefully acknowledged.

References

- Abrams DP, Angel R, Uzarski J (1996) Out-of-plane strength of unreinforced masonry infill panels. *Earthquake Spectra* 12(4):825–844
- ACI (2011) Building code requirements for reinforced concrete. American Concrete Institute Structural Journal DOI 30CFR250.901(d)(1)
- Akhoundi F, Vasconcelos G, Lourenço PB, Palha CAO, Martins A (2015) Out-of-plane behavior of masonry infill walls. In: 7th International Conference on Seismology & Earthquake Engineering
- Akhoundi F, Vasconcelos G, Lourenço PB, Silva L (2016) Out-of-plane response of masonry infilled rc frames: Effect of workmanship and opening. In: 16th International Brick and Block Masonry Conference "Masonry in a world of challenges", Taylor & Francis, pp 1147–1154
- Al Hanoun M, Abrahamczyk L, Schwarz J (2018) Macromodeling of in-and out-of-plane behavior of unreinforced masonry infill walls. *Bulletin of Earthquake Engineering* pp 1–17
- Anderson C, Bright N (1976) Behavior of non-loadbearing block walls under windloading. *Concrete* 10(9):27–30
- Angel R, Abrams DP, Shapiro D, Uzarski J, Webster M (1994) Behavior of reinforced concrete frames with masonry infills. Tech. rep., University of Illinois Engineering Experiment Station. College of Engineering. University of Illinois at Urbana-Champaign.
- Anić F, Penava D, Guljaš I, Sarhosis V, Abrahamczyk L, Butenweg C (2018) The effect of openings on out-of-plane capacity of masonry infilled reinforced concrete frames. In: 16th European Conference on Earthquake Engineering
- Anić F, Penava D, Abrahamczyk L, Sarhosis V (2019) Computational evaluation of experimental methodologies of out-of-plane behavior of framed-walls with openings. *Earthquakes and Structures* 16(3):265
- Arêde A, Furtado A, Melo J, Rodrigues H, Varum H, Pinto N (2017) Challenges and main features on quasi-static cyclic out-of-plane tests of full-scale infill masonry walls. In: Conference: 7th International Conference on Advances in Experimental Structural Engineering
- Asteris P, Cavaleri L, Di Trapani F, Tsaris A (2017) Numerical modelling of out-of-plane response of infilled frames: State of the art and future challenges for the equivalent strut macromodels. *Engineering Structures* 132:110–122, DOI 10.1016/j.engstruct.2016.10.012
- Bashandy TW (1995) Behavior of reinforced concrete infilled frames under dynamic loading: Part 1. Master's thesis, The University of Texas at Austin, mS thesis
- Benedetti D, Benzonì G (1984) A numerical model for seismic analysis of masonry buildings: Experimental correlations. *Earthquake engineering & structural dynamics* 12(6):817–831
- Booth E, Key D (2006) *Earthquake Design Practice for Buildings*. Thomas Telford, London, URL <http://ebooks.cambridge.org/ref/id/CB09781107415324A009>
- BSI (2004) Eurocode 6: Design of masonry structures—Part 1–1: Common rules for reinforced and unreinforced masonry structures. ENV 1996-1-1: 2004: E, CEN Brussels
- BSI (2005) Eurocode 8: Design of structures for earthquake resistance-part 1: general rules, seismic actions and rules for buildings. British Standards Institution
- CAEE (1984) Colombian standards for seismic resistant design and construction nsr-84. Tech. rep., Colombian Association for Earthquake Engineering, Bogota, Colombia
- Canadian Standards Association and Standards Council of Canada (1978) *Masonry design and construction for buildings*. 1977, The Association

- CNIC (1988) Venezuelan seismic code, 1988. regulations for earthquake resistant buildings. Comision De Normas Industriales, Covenin
- Committee MSJ, et al. (1999) Building code requirements for masonry structures. American Concrete Institute, Detroit, MI, ISBN 1929081022
- Dawe J, Seah C (1989) Out-of-plane resistance of concrete masonry infilled panels. *Canadian Journal of Civil Engineering* 16(6):854–864
- Domenico MD, Ricci P, Verderame GM (2018) Experimental assessment of the influence of boundary conditions on the out-of-plane response of unreinforced masonry infill walls. *Journal of Earthquake Engineering* 0(0):1–39, DOI 10.1080/13632469.2018.1453411, URL <https://doi.org/10.1080/13632469.2018.1453411>
- Drysdale R, Essawy A (1988) Out-of-plane bending of concrete block walls. *Journal of Structural Engineering-asce - J STRUCT ENG-ASCE* 114
- EERI (2018) Earthquake engineering research institute. <https://www.eeri.org/>, accessed: 30/10/2018
- FEMA 273 (1997) Guidelines for the seismic rehabilitation of buildings. Tech. rep., Federal Emergency Management Agency Washington, DC
- FEMA 356 (2000) Commentary for the seismic rehabilitation of buildings. FEMA-356, Federal Emergency Management Agency, Washington, DC
- Flanagan R (1994) Behavior of structural clay tile infilled frames. Tech. rep., Center for natural phenomena engineering
- Flanagan RD, Bennett RM (1999a) Arching of masonry infilled frames: Comparison of analytical methods. *Practice Periodical on Structural Design and Construction* 4(3):105–110
- Flanagan RD, Bennett RM (1999b) Bidirectional behavior of structural clay tile infilled frames. *Journal of Structural Engineering* 125(3):236–244, DOI 10.1061/(ASCE)0733-9445(1999)125:3(236)
- Fowler JJ (1994) Analysis of dynamic testing performed on structural clay tile infilled frames. PhD thesis, Oak Ridge National Lab.(ORNL), Oak Ridge, TN (United States)
- Furtado A, Rodrigues H, Arède A, Varum H (2015) Experimental Characterization of the In-plane and Out-of-Plane Behaviour of Infill Masonry Walls. *Procedia Engineering* 114:862–869, DOI 10.1016/j.proeng.2015.08.041, URL <http://linkinghub.elsevier.com/retrieve/pii/S187770581501680X>
- Furtado A, Rodrigues H, Arède A, Varum H (2016) Simplified macro-model for infill masonry walls considering the out-of-plane behaviour. *Earthquake Engineering & Structural Dynamics* 45(4):507–524
- Furtado A, Rodrigues H, Arède A, Varum H (2018a) Effect of the panel width support and columns axial load on the infill masonry walls out-of-plane behavior. *Journal of Earthquake Engineering* 0(0):1–29, DOI 10.1080/13632469.2018.1453400, URL <https://doi.org/10.1080/13632469.2018.1453400>
- Furtado A, Rodrigues H, Arède A, Varum H (2018b) Out-of-plane behavior of masonry infilled rc frames based on the experimental tests available: A systematic review. *Construction and Building Materials* 168:831–848
- Gabrielsen B, Wilton C, Kaplan K (1975) Response of arching walls and debris from interior walls caused by blast loading. Tech. rep., URS RESEARCH CO SAN MATEO CA
- Griffith M, Vaculik J (2007) Out-of-plane flexural strength of unreinforced clay brick masonry walls. *TMS Journal* 25:53–68
- Griffith MC, Vaculik J, Lam NTK, Wilson J, Lumantarna E (2007) Cyclic testing of unreinforced masonry wall in two way bending. *Earthquake Engineering & Structural Dynamics* 36(6):801–821, DOI 10.1002/eqe.654, URL <https://onlinelibrary.wiley.com/doi/abs/10.1002/eqe.654>
- Hak S, Morandi P, Magenes G (2014) Out-of-plane experimental response of strong masonry infills. In: 2nd European Conference on Earthquake Engineering and Seismology
- Hallquist Å (1970) Lateral loads on masonry walls. Norwegian building research institute Reprint from the Symposium on bearing walls, Warsaw 1969
- Haseltine BA (1976) Design of laterally loaded wall panels. *Proceedings of the British Ceramic Society* pp 115–126
- Hashemi SA, Mosalam KM (2007) Seismic evaluation of reinforced concrete buildings including effects of masonry infill walls
- Henderson R, Jones W, Burdette E, Porter M (1993) The effect of prior out-of-plane damage on the in-plane behavior of unreinforced masonry infilled frames. In: *The Fourth DOE Natural Phenomena Hazards Mitigation Conference*
- Hendry AW (1973) Lateral strength of unreinforced brickwork. *Structural Engineer* 51(2):43–50
- Holmes M (1961) Steel frames with brickwork and concrete infilling. In: *Proceedings of Institution of Civil Engineers*, DOI 10.1680/jicep.1961.11305
- Howe G (1936) Behavior of non-loadbearing block walls under windloading
- INEN (2001) Código ecuatoriano de la construcción – requisitos generales de diseño (inen-5). Instituto Ecuatoriano de Normalización
- IS 1893 (2002) IS 1893: Indian standard criteria for earthquake resistant design of structures: Part 1 general provisions and buildings
- Jäger W, Vassilev T, Hoffmann J, Schöps P (2008) Unreinforced masonry basement walls—a comparison of theoretical design approaches and numerical simulations. In: *Proceedings of the 14th International Brick & Block Masonry Conference*. The University of Newcastle, Sydney/Australia, p 68
- Klingner R, Rubiano N, Bashandy T, Sweeney S (1996) Evaluation and analytical verification of shaking table data from infilled frames, part 2: Out-of-plane behavior. In: *Proceedings of the 7th North American Masonry Conference*, Colorado: Elsevier Science Ltd, pp 521–532
- Komaraneni S, Rai DC, Singhal V (2011) Seismic behavior of framed masonry panels with prior damage when subjected to out-of-plane loading. *Earthquake Spectra* 27(4):1077–1103
- Lam N, Griffith M, Wilson J, Doherty K (2003) Time–history analysis of urm walls in out-of-plane flexure. *Engineering Structures* 25(6):743–754, DOI [https://doi.org/10.1016/S0141-0296\(02\)00218-3](https://doi.org/10.1016/S0141-0296(02)00218-3), URL <http://www.sciencedirect.com/science/article/pii/S0141029602002183>
- Liu M, Cheng Y, Liu X (2011) Shaking table test on out-of-plane stability of infill masonry wall. *Transactions of Tianjin University* 17(2):125
- Mays GC, Hetherington JG, Rose TA (1998) Resistance-deflection functions for concrete wall panels with openings. *Journal of Structural Engineering* 124(5):579–587, DOI 10.1061/(ASCE)0733-9445(1998)124:5(579), URL <https://ascelibrary.org/doi/abs/10.1061/%28ASCE%290733-9445%281998%29124%3A5%28579%29>
- McDowell E, McKee K, Sevin E (1956a) Arching action theory of masonry walls. *Journal of the Structural Division* 82(2):1–8

- McDowell E, McKee K, Sevin E (1956b) Discussion of arching action theory of masonry walls. *Journal of the Structural Division* 82:27–40
- MHPP (1995) Nepal national building code for seismic design of buildings in nepal (nbc-105). Ministry of Housing and Physical Planning, Department of Buildings
- Misir IS, Ozelcik O, Girgin SC, Yucel U (2016) The behavior of infill walls in rc frames under combined bidirectional loading. *Journal of Earthquake Engineering* 20(4):559–586, DOI 10.1080/13632469.2015.1104748
- Moghaddam H, Goudarzi N (2010) Transverse resistance of masonry infills. *ACI Structural Journal* 107(4):461
- Monk CB (1958) Resistance of Structural Clay Masonry to Dynamic Forces: A Design Manual for Blast Resistance. 7, Structural Clay Products Research Foundation
- Mosoarca M, Petrus C, Stoian V, Anastasiadis A (2016) Behaviour of masonry infills subjected to out of plane seismic actions. part 2: Experimental testing. In: 16th International Brick and Block Masonry Conference
- NCH (1996) Earthquake-resistant design of buildings nch 433. National Institute of Normalization
- NSCP (1992) National structural code of philippines, vol. 1, fourth edition (nscp). The Board of Civil Engineering of the Professional Regulation Commission
- NTS (1997) National technical standard e-030 “earthquake resistant design”. Ministry of Transportation, Communications and Housing
- NZS-3101 (1995) Code of practice for the design of concrete structures, part 1 (nzs-3101). Tech. rep., Standards Association of New Zealand, Wellington, New Zealand
- Pasca M, Liberatore L, Masiani R (2017) Reliability of analytical models for the prediction of out-of-plane capacity of masonry infills. *Structural Engineering and Mechanics* 64(6):765–781
- Penava D, Sigmund V (2017) Out-of-plane behaviour of framed-masonry walls with opening as a result of shaking table tests. In: 16th World Conference on Earthquake Engineering
- Pereira J, Campos J, Lourenço P (2014) Experimental study on masonry infill walls under blast loading. In: The 9th International Masonry Conference
- Pereira MFP, Pereira M, Ferreira J, Lourenço PB (2011) Behavior of masonry infill panels in rc frames subjected to in plane and out of plane loads. In: 7th International Conference on Analytical Models and New Concepts in Concrete and Masonry Structures
- Petrus C, Stoian V, Marius M, Anastasiadis A (2015) Reinforced concrete frames with masonry infills. out of plane experimental investigation. *Acta Technica Napocensis*
- da Porto F, Guidi G, Dalla Benetta M, Verlato N (2013) Combined in-plane/out-of-plane experimental behaviour of reinforced and strengthened infill masonry walls. In: Proceedings of 12th Canadian Masonry Symposium
- Preti M, Bettini N, Plizzari G (2012) Infill walls with sliding joints to limit infill-frame seismic interaction: Large-scale experimental test. *Journal of Earthquake Engineering* 16(1):125–141, DOI 10.1080/13632469.2011.579815
- Preti M, Migliorati L, Giuriani E (2015) Experimental testing of engineered masonry infill walls for post-earthquake structural damage control. *Bulletin of Earthquake Engineering* 13(7):2029–2049, DOI 10.1007/s10518-014-9701-2, URL <http://link.springer.com/10.1007/s10518-014-9701-2>
- Quintas V (2003) Two main methods for yield line analysis of slabs. *Journal of Engineering Mechanics-asce - J ENG MECH-ASCE* 129
- Rabinovitch O, Madah H (2011) Finite element modeling and shake-table testing of unidirectional infill masonry walls under out-of-plane dynamic loads. *Engineering Structures* 33(9):2683 – 2696, DOI <https://doi.org/10.1016/j.engstruct.2011.05.019>
- Reindl L, Butenweg C, Kubalski T (2011) Numerical simulation of unreinforced masonry walls subject to dynamic out-of-plane loading. In: Proceedings of the 3rd International Conference on Computational Methods in Structural Dynamics and Earthquake Engineering, pp 25–28
- Rupakhety R, Ólafsson S (2018) *Earthquake Engineering and Structural Dynamics in Memory of Ragnar Sigbjörnsson, Geotechnical, Geological and Earthquake Engineering*, vol 44. Springer International Publishing, Cham, DOI 10.1007/978-3-319-62099-2, URL <https://link.springer.com/content/pdf/10.1007/978-3-319-62099-2.pdf><http://link.springer.com/10.1007/978-3-319-62099-2>
- Sepasdar R (2017) Experimental investigation on the out-of-plane behaviour of concrete masonry infilled rc frames. Master’s thesis, Dalhousie University
- Shapiro D, Uzarski J, Webster M, Angel R, Abrams DP (1994) Estimating out-of-plane strength of cracked masonry infills. Tech. rep., University of Illinois Engineering Experiment Station. College of Engineering. University of Illinois at Urbana-Champaign.
- SI (1995) Design provisions for earthquake resistance of structure (si-413). The Standards Institution of Israel
- Sigmund V, Penava D (2014) Influence of openings, with and without confinement, on cyclic response of infilled r-c frames — an experimental study. *Journal of Earthquake Engineering* 18(1):113–146, DOI 10.1080/13632469.2013.817362, URL <https://doi.org/10.1080/13632469.2013.817362>, <https://doi.org/10.1080/13632469.2013.817362>
- Smith NL, Tait MJ, El-Dakhkhni WW, Mekky WF (2016) Response analysis of reinforced concrete block infill panels under blast. *Journal of Performance of Constructed Facilities* 30(6):04016059, DOI 10.1061/(ASCE)CF.1943-5509.0000825
- SNiP (1995) Building code on construction in seismic areas (snip-ii-7–81). The Ministry for Construction of Russia
- de Sousa H (2014) Typical masonry wall enclosures in portugal. *Enclosure Masonry Wall Systems Worldwide: Typical Masonry Wall Enclosures in Belgium, Brazil, China, France, Germany, Greece, India, Italy, Nordic Countries, Poland, Portugal, the Netherlands and USA* p 179
- Surendran S, Kaushik HB (2012) Masonry infill rc frames with openings: review of in-plane lateral load behaviour and modeling approaches. *The open construction and building technology journal* 6(Suppl. 1-M9):126–154
- Tasnimi A, Mohebkah A (2011) Investigation on the behavior of brick-infilled steel frames with openings, experimental and analytical approaches. *Engineering Structures* 33(3):968–980
- Tools for Engineer website (2019) Tools for engineer. <http://www.toolsforengineer.com/>, accessed: 13/02/2019
- Tu YH, Chuang TH, Liu PM, Yang YS (2010) Out-of-plane shaking table tests on unreinforced masonry panels in rc frames. *Engineering Structures* 32(12):3925 – 3935, DOI <https://doi.org/10.1016/j.engstruct.2010.08.030>, URL <http://www.sciencedirect.com/science/article/pii/S014102961000341X>
- Ugural AC, Fenster SK (2003) *Advanced strength and applied elasticity*. Pearson Education

- Vaculik J (2012) Unreinforced masonry walls subjected to out-of-plane seismic actions. PhD thesis, The University of Adelaide; School of Civil, Environmental & Mining Engineering
- Varela-Rivera J, Polanco-May M, Fernandez-Baqueiro L, I Moreno E (2012) Confined masonry walls subjected to combined axial loads and out-of-plane uniform pressures. *Canadian Journal of Civil Engineering* 39:439–447
- VBS (2006) Vietnamese seismic design standard tcxdvn 375:2006. Tech. rep., Vietnamese Building Standard, Hanoi, Vietnam
- Verlato N, Guidi G, da Porto F, Modena C (2016) Innovative systems for masonry infill walls based on the use of deformable joints: combined in-plane/out-of-plane tests. In: *Proceedings of the 16th International Brick and Block Masonry Conference*
- Wang C (2017) Experimental investigation on the out-of-plane behaviour of concrete masonry infilled frames
- Wilton C, Gabrielsen BL (1973) Shock tunnel tests of preloaded and arched wall panels. Tech. rep., URS RESEARCH CO SAN MATEO CALIF
- Yuen Y, Kuang J (2012) Effect of out-of-plane loading on lateral force transfer mechanisms of infilled rc frames. In: *14th International Conference on Computing in Civil and Building Engineering*